2011

COMPARATIVE STUDY OF 3D TISSUE ENGINEERING SCAFFOLD FABRICATION METHODS

Lisa Rogers

COMPARATIVE STUDY OF 3D TISSUE ENGINEERING SCAFFOLD FABRICATION METHODS

(Spine title: Comparative Study of Scaffold Fabrication Methods)

(Thesis Format: Monograph)

by

Lisa Rogers

Graduate Program in Engineering Science
Department of Chemical and Biochemical Engineering

Submitted in partial fulfilment
of the requirements for the degree of
Master of Engineering Science

School of Graduate and Postdoctoral Studies
The University of Western Ontario
London, Ontario

Abstract

Tissue engineering scaffolds act as a structural template for seeded cells and play a significant role in dictating the performance of the final tissue construct. Scaffold properties are governed by the fabrication method and must be tailored to meet the intended application. In this work, 3D poly(carbonate) urethane (PCU) scaffolds were fabricated by solvent casting/particulate leaching (SCPL) and electrospinning. For SCPL, three different types of porogens, namely, alginate beads, D-fructose particles, and gelatin spheres were used. The effects of porogen type and fabrication method on scaffold morphological characteristics were examined. Highly porous scaffolds with uniform pore morphology were fabricated using all three porogen types, and fibrous scaffolds having an average fiber diameter of ~200 nm were fabricated by electrospinning. Preliminary cell culture studies carried out with vascular smooth muscle cells indicated that electrospun scaffolds and scaffolds fabricated by SCPL using alginate beads and D-fructose were not cytotoxic and provided a favorable environment for cell growth.

Keywords: Polyurethane, scaffold, solvent casting/particulate leaching, electrospinning, porogen, alginate beads, D-fructose, gelatin spheres, vascular smooth muscle cells.

Acknowledgments

I would like to extend my sincere gratitude to my supervisor, Dr. Kibret Mequanint, whom I have had the pleasure of working with throughout the course of my studies at The University of Western Ontario, and whose guidance and advice had been invaluable. Thank you to Dr. Shigang Lin for his help with the cell studies and to the rest of the Mequanint lab members for their input and support. Thank you also to Dr. Joseph Umoh from the Robarts Research Institute for his help with the MicroCT analysis. I would also like to acknowledge the Natural Sciences and Engineering Research Council of Canada (NSERC) and The Ontario Graduate Scholarship (OGS) program for providing scholarships during my research. Last, but not least, I wish to thank my parents for their continued support and encouragement.

Table of Contents

List of Figures

List of Tables

List of Abbreviations

DMF	Dimethylformamide
DMSO	Dimethylsulfoxide
ECM	Extracellular matrix
EDTA	Ethylenediaminetetraacetic acid
HCASMCs	Human coronary artery smooth muscle cells
HLB	Hydrophile Lipophile Balance
MicroCT	Microcomputed tomography
PCU	Poly(carbonate urethane)
PEG	Polyethylene glycol
PGA	Poly(glycolic acid)
PI	Phase inversion
PLLA	Poly-L-Lactic Acid
SCPL	Solvent casting/particulate leaching
SEM	Scanning Electron Microscopy

CHAPTER 1

1 Scope and Thesis Outline

1.1 Overall Objectives and Rationale

At its central tenet, tissue engineering involves the *in vitro* seeding and attachment of cells onto three-dimensional (3D) scaffolds. These cells then migrate, proliferate, and differentiate into the intended specific tissues while secreting the extracellular matrix (ECM) components required for support and tissue morphogenesis. It is evident, therefore, that the choice of scaffold is crucial to enable the cells to behave in the required manner to produce tissues and organs of the desired shape and size.[1] Engineered tissues eliminate many of the problems that are faced when using donor organs or synthetically made devices for therapeutic applications. The morphological and mechanical properties of tissue engineered biomaterial constructs should closely resemble those of the tissue they intend to replace.[2] Thus, the success of engineered constructs largely depends on the said properties of the scaffold, which supports the survival, proliferation, and differentiation of seeded cells. Engineering scaffolds provide the supporting structure needed for cells to organize in 3D and form a tissue. Scaffolds can be biodegradable or biostable and their properties are dependent on the intended application. However, in general, they should be biocompatible and highly porous in order to allow for cell ingrowth. Scaffold properties are greatly dependent on the fabrication technique, and there are a vast number of techniques that have been

reported, each with advantages and disadvantages. In this work, a comparative study of scaffold fabrication techniques was carried out in order to evaluate the effect of the fabrication method on the morphological properties of the scaffold, and to assess the suitability of the techniques for vascular tissue engineering applications.

1.2 Thesis Layout

This thesis has 5 Chapters. Chapter 2 introduces the concept of tissue engineering, discusses the importance of vascular tissue engineering, and provides a comprehensive review of the scaffold fabrication techniques reported in the literature thus far. The specific objectives of this project are also provided at the end of Chapter 2. Chapter 3 details the experimental procedures, while Chapter 4 presents and discusses the results of this study. Finally, the important findings and future directions are summarized in Chapter 5.

CHAPTER 2

2 Introduction

2.1 Tissue Engineering

In accordance with one of the most widely accepted definitions,[3] tissue engineering is an interdisciplinary field that applies the principles of engineering and life sciences to the development of biological substitutes that restore, maintain, or improve tissue function or a whole organ. The main objective of tissue engineering is to aid tissue formation or regeneration of diseased or damaged organs through the use of cultured human cells or through the recruitment of endogenous cells, and thereby provide therapeutic or diagnostic benefit.[4,5]

There are four main tissue engineering approaches: cell transplantation, scaffold implantation, cell-seeded scaffold implantation, and *in vitro* tissue engineering.[4] *In vitro* tissue engineering is the most frequent approach whereby cells are seeded onto a supporting structure known as a scaffold and the construct is then cultured in a bioreactor before implantation in the body as a replacement. In some applications, this approach is modified such that certain steps from the general procedure are omitted. For example, in myocardial tissue regeneration, cardiac muscle cells can be directly injected into the heart tissue to repair damaged myocardium.[6] This is the cell transplantation approach. In other cases such as vascular intervention, natural or synthetic grafts are directly implanted into the host such that the cell-seeding and *in*

vitro maturation step are omitted.[7] This is known as the scaffold implantation approach whereby endogenous cells are prompted to invade the uncellularized construct. Finally, in the cell-seeded implantation approach, only the *in vitro* maturation step is omitted, such as in the case of endothelial cell-seeding of vascular grafts.[8]

The first commercial application of engineered tissue was a bioartificial skin product for burn treatment that was introduced in 1990.[9] Engineered tissues such as blood vessels,[10] bladder[11] and trachea[12] have already seen success and are used to some extent clinically.

2.2 Why Vascular Tissue Engineering?

Vascular disease is the leading cause of mortality in Western Societies. The body's vasculature maintains homeostasis, regulates blood flow, and provides necessary nutrients and oxygen exchange to all parts of tissues.[13] As a result, diseases that affect the function of blood vessels are often serious and life threatening.

Although minimally invasive surgeries such as angioplasty and stenting are frequent, vascular intervention often involves the surgical implantation of grafts. The use of saphenous vein, internal mammary artery, and radial artery as autologous bypass grafts is the mainstay of revascularization for ischemic heart disease and peripheral vascular disease.[7, 14] Each year over 500,000 patients in USA, 220,000 in Western Europe and 23,000 Canadians undergo coronary artery bypass grafting operations.[15,16]

As the elderly segment of the population increases, the numbers of coronary and peripheral vascular interventions are expected to increase. However, 20%–30% of patients who require coronary artery bypass grafting do not have suitable autologous vessels for the procedure.[17] Allograft and xenograft vascular substitutes provide an alternative but often result in immune rejection, poor patency, and compliance mismatch.[16]

Synthetic materials such as polyethylene terephathalate (PET, Dacron®) and polytetrafluoroethylene (PTFE) have been used for treatment of coronary and peripheral vascular disease, but they are limited to high-flow/low-resistance conditions because of poor elasticity, low compliance, and thrombogenicity of synthetic surfaces.[14] Thus, small-diameter synthetic vascular grafts (internal diameter less than 5 mm) have shown poor patency rates.[7] In addition, synthetic grafts often fail due to immune-mediated rejection by the host.[16] Synthetic materials also lack growth potential.[7] Furthermore, none of the aforementioned therapies provide permanent solutions. The goal of vascular tissue engineering is, therefore, to resolve the problems associated with these approaches.

A tissue engineered vascular graft offers many advantages such as its inherent healing potential and ability to be remodeled by the body according to the needs of the environment.[5] In the *in vitro* tissue engineering approach, vascular cells may be seeded onto biodegradable scaffolds *ex vivo* and allowed to remodel before transplantation. As the cells organize in three-dimensions and synthesize their own

natural ECM, the scaffold degrades, leaving only the natural tissue. Despite the advantages of tissue engineered vascular grafts, there are also substantial challenges faced with this approach. Difficulties arise in designing a biomaterial that retains seeded vascular cells while maintaining morphological and phenotypical characteristics.[18] In addition, while some engineered tissues may rely on remodeling of the tissue in vivo, tissue engineered vascular substitutes must be immediately functional upon implantation, since premature substitutes lead to catastrophic failure.[16] A functional tissue engineered blood vessel should also be nonthrombogenic, nonimmunogenic, and have viscoelasticity similar to that of native vessels.[19]

Engineered vascular tissues have not only clinical significance but also the potential to be used in diagnostic applications for testing drug uptake and metabolism, toxicity, as well as pathogenicity contributing to our understanding of genetic or environmental factors regulating treatment outcomes. The use of cell and organ culture in combination with animal models to study vascular diseases (e.g. atherosclerosis, post angioplasty restenosis, and hypertension) with the goal of developing therapeutics is not new, but employing engineered human vascular tissues for this role is a novel concept.[20, 21] Although conventional 2D cell cultures are neccesary to our understanding of tissue morphogenesis and function in physiological and pathological states, they do not accurately replicate the 3D microenvironment of human tissues. For example, 2D culturing of vascular cells for studying intimal hyperplasia without the arterial wall structure and ECM cannot recapitulate the

intricate vascular wall mechanics and morphogenesis.[20, 22] Similarly, animal organ cultures and whole animal models do not completely mimic the human biology due to inevitable inter-species differences. Studies using closely related nonhuman primates are constrained by limited availability, legal restrictions, ethical concerns, and high cost.[20]

The most realistic model when studying human vascular diseases and therapeutics is obviously that of a human tissue, but the inability to experiment directly on human subjects limits this progress. As such, the need for an engineered human vascular tissue model to close this gap is of vital importance. Although engineered vascular tissues are not likely to replace animal or human subjects, they have the potential to provide high throughput of substantive and detailed information regarding specific conditions under controlled environments. The significance is far-reaching as these "made to order" vascular tissues comprising cells (smooth muscle and endothelial cells) and ECM (elastin and collagen) could serve as a powerful high-throughput tool to study disease models and therapeutic outcomes that are not possible with animal-based models.[23, 24] In this context, engineered vascular tissue technology may be used both to validate drug targets and to optimize loads. This allows for cardiovascular drug screening in a more controlled and efficient way than can be performed using a traditional whole animal approach, thereby minimizing the number of laboratory animals used and decreasing the overall cost of performing research.[23] The use of 3D engineered tissue to reduce the cost and time required for physiological genomic research is another niche which is unexplored. Recently engineered 3D tissues such as

cardiac patch,[25] lung tissue,[26] cornea,[27] and solid tumor models[28] have emerged as powerful tools for drug discovery and to study cells in 3D.[29] In comparison with 2D cultures, 3D cell models create a more realistic representation of real tissues, which is critical for many important cell functions, including morphogenesis, cell metabolism, gene expression, differentiation, and cell-cell interactions.[29] In view of this, 3D scaffolds play a role in vascular tissue engineering platforms.

2.3 Tissue Engineering Scaffolds

Primary cells are anchorage-dependant and require specific environments, meaning a supporting material is needed to act as a template for survival and growth.[30] Tissue engineering scaffolds are used for this purpose. The scaffold should promote cell adhesion, proliferation, and ECM production. That is, the scaffold should surrogate the missing ECM.[31] With the exception of a few cases,[5, 32-36] tissue engineering strategies rely on appropriate scaffolds. Scaffolds are basically three-dimensional structural templates to support cell adhesion, migration, differentiation, proliferation and provide guidance for neo tissue formation.[37, 38] Ideally, after fulfilling their function as a template, they should degrade into nontoxic byproducts. The coordinated rates of scaffold degradation and neo tissue generation are essential elements to be considered.[39]

2.3.1 Scaffold Properties

An ideal tissue engineering scaffold should mimic the structure and biological function of native ECM in terms of both chemical composition and physical structure. Native ECM does much more than just provide a physical support for cells. It also provides a substrate with specific ligands for cell adhesion and migration. Furthermore, it provides various growth factors, which regulate cellular proliferation and function.[40] Thus, a scaffold needs to provide both contact guidance cues, which direct the development and alignment of cells, as well as biochemical cues, which direct compositional and organizational changes in the construct.[7]

A scaffold should be biocompatible, and, in most cases, biodegradable. The scaffold degradation rate should coordinate with extracellular matrix deposition carried out by the cells in order to guarantee the required support during tissue formation.[31] Scaffolds also need to possess appropriate mechanical properties in order to provide the appropriate stress environment for the neotissue.[30] The rate of degradation and mechanical properties of the scaffold are linked to the degree of porosity. There is a trade-off between high porosity and mechanical strength of the scaffold.

Architecture and porosity are two other required features for tissue engineering. Scaffold architecture should be such that it permits cell infiltration, nutrient and waste product permeation, and new capillary network formation.[31] This architecture is believed to play a significant role in the development of specific biological functions in tissues while providing appropriate nutritional conditions and spatial organization

for cell growth.[30] Spatial cellular organization determines cell–cell and cell–matrix interactions and is critical to tissue and organ function.[41] It is also important that the pore architecture be uniform and that the pores be interconnected. Tissues generated from nonuniform pore architectures have shown inferior biomechanical properties when compared with scaffolds having a uniform pore structure.[31] Interconnected pores are important because transport of materials and cell migration is inhibited if the pores are not interconnected, even if the porosity is high.[42]

Scaffold porosity is equally a required characteristic for the regeneration of tissues. High porosity (70-95%) and surface-area-to-volume ratio is desired. High surface area is beneficial for cell attachment and anchorage, while high pore volume enables cell growth, migration, and transport of fluids and nutrients.[31] More specifically, microporosity is important for capillary ingrowth and interactions between the cells and matrix, while macroporosity is more important for nutrient supply and waste removal of cell metabolism.[31] Pore size and shape can also affect tissue ingrowth.[43] The optimal pore size range is strictly connected to the tissue type, but when the pore size is too small, pore occlusion can occur, preventing cell penetration.[44] Finally, scaffolds also require appropriate surface structure and chemistry for cell attachment, and often chemical or physical surface modifications are imparted to enhance cell-material interactions.

2.3.2 Scaffold Materials

Both naturally occurring and synthetic materials are available to fabricate scaffolds. Developing materials for tissue engineering scaffolds is often challenging since they must have specific mechanical and bioresorbable properties as well as being suited for various fabrication processes. The choice of material for tissue engineering scaffolds depends on the application. In general, it is not possible to meet all criteria by a particular scaffold material since biological and synthetic scaffolds have both advantages and disadvantages (see Table 1).

Table 1: Properties of biological and synthetic scaffolds.[45]

	Biological Scaffolds	Synthetic Scaffolds
Advantages	▪ Naturally occurring, nontoxic ▪ Favorable for cell binding. ▪ Generally biocompatible.	▪ Precise control over material properties. ▪ Easily available and cheap. ▪ Easy to process. ▪ Little or no batch-to-batch variations.
Disadvantages	▪ May degrade rapidly. ▪ Weak mechanical property unless crosslinked. ▪ Inconsistency between different batches. ▪ Risk of disease transmission.	▪ Toxic residual monomers or catalysts and degradation byproducts may illicit inflammation. ▪ Poor cellular interaction.

For hard tissue applications such as bone and teeth, ceramics, composites, and rigid polymers have been widely used as scaffold materials, while for soft tissues such as skin, tendon, and blood vessels, soft natural or synthetic polymers have been used.[46] Natural polymers, such as collagens, glycosaminoglycan, starch, chitin, and chitosan, have been used to repair nerves, skin, cartilage, and bone.[30] Although naturally occurring polymers offer great potential due to their biocompatibility, they cannot be easily mass-produced, and concerns about finding the large amounts of material needed for clinical applications have led to the investigation of synthetic polymers for use as scaffold materials.[47]

Synthetic polymers can be easily mass-produced, and their properties can be tailored for specific applications. Most of these polymers can be designed to undergo simple hydrolytic degradation reactions.[31] The degradable polymers that are most used as scaffold materials are poly(glycolic acid) (PGA), poly(lactic acid) (PLA), and their copolymer, poly(DL-lactic-co-glycolic acid) (PLGA), as well as the aliphatic polyester polycaprolactone (PCL).[31]

Although not strictly biodegradable, polyurethanes have excellent physical properties and good biocompatibility, making them good candidates for many biomedical applications.[7] They were first used in the early 1950s for foam breast implants and cardiovascular devices.[31] They have also been used in applications such as pacemakers, catheters, and heart valves. For all of these applications, biostable polyurethanes were used. The favorable mechanical properties of polyurethanes has

led to considerable research aimed at their use as scaffolds for the development of vascular grafts.[7]

2.3.3 Scaffold Fabrication Techniques

When designing scaffolds for tissue engineering, the desired chemical and physical properties, as well as the reproducibility, cost-effectiveness, and ability to include biological components during processing should be considered. There are many different scaffold fabrication techniques that have been developed, each with advantages and disadvantages. Brief reviews of these different techniques are presented here.

2.3.3.1 Fiber Meshes and Fiber Bonding

Some of the first scaffolds used to demonstrate the feasibility of tissue regeneration were made from non-woven fibers in the form of tassels and felts.[48] Scaffolds were also prepared such that fibers were woven or knitted into 3D patterns of variable pore size. Advantages of these fiber meshes include large surface area for cell attachment and rapid diffusion of nutrients. However, their structure lacked the stability needed for *in vitro* use. This led to the development of the fiber bonding technique.[48,49] There are two different fiber bonding techniques. In the first technique,[48] polymer fibers (polymer A) are immersed in a solution consisting of a second polymer (polymer B) and a solvent that is a non-solvent for polymer A. The solvent is evaporated, resulting in the formation of a polymer-polymer composite, whereby the network of polymer A

fibers is embedded in polymer B. When heating the composite to above the melting point of both polymers, polymer B melts first, filling all voids left by the fibers. As polymer A begins to melt, fibers at the cross-points become 'welded' together, and polymer B is then removed by dissolution. Foams with porosities as high as 81% and pore diameters of up to 500 μm were produced with this technique. In the second fiber bonding technique,[50] polymer A fibers are bonded by coating them using atomization of polymer B, whereby fibers are sprayed with a solution of polymer B. The fibers remain unchanged during this process, and following solvent evaporation the fibers are glued together. Similar pore sizes were obtained with this technique.

Although these fiber bonding approaches produced highly porous scaffolds with interconnected pores, there are several disadvantages that limit their use. First, fine control of porosity is difficult. Second, the choice of solvent, immiscibility of the two polymers, and their relative melting temperatures restricts the choice of polymers that can be used. Finally, the use of toxic chemicals and extreme temperatures (in the case of the first fiber bonding technique) makes it difficult to include cells or bioactive molecules, such as growth factors, during processing.[47]

2.3.3.2 Gas Foaming

Gas foaming was developed to eliminate the need for organic solvents.[42] In this process, solid polymer (PGA, PLLA, or PLGA) discs are prepared using compression molding with a heated mold. The discs are then placed in a chamber and exposed to

high pressure carbon dioxide for several days. The pressure is then rapidly reduced to atmospheric pressure. Porosities of up to 93% have been achieved by this technique, but the pores are largely unconnected, especially on the surface of the foam.[47]

2.3.3.3 Phase Separation

Phase separation is frequently used in the preparation of 3D tissue engineering scaffolds. In this technique, phase separation of a polymer solution is induced, creating polymer-rich and solvent-rich domains within the solution. This is created by quenching under low temperatures. Following solvent removal by freeze-drying, porous polymer scaffolds are produced. If phase separation is induced by changing the temperature, it is known as thermally-induced phase separation, while if it is induced by adding a non-solvent to the polymer solution, it is known as non-solvent-induced phase separation.[51] Scaffolds with porosities of up to 95% have been fabricated with the phase separation method.[52] These scaffolds usually have a spongelike porous morphology with microscale spherical pores.[53] However, the morphology can be altered by changing parameters such as the type of polymer used, polymer concentrations, solvent/non-solvent ratio, and thermal quenching strategy.[30] For example, the phase separation technique has been used to fabricate nanofibrous scaffolds with fiber diameters ranging from 50 to 500 nm.[54,41]

Although the ability to tailor pore size and porosity by altering process parameters is appealing, in practice, the phase separation technique is so sensitive to process variations that precise control of scaffold morphology is difficult.[52] In addition, this

technique is limited to small pores.

2.3.3.4 Emulsification/Freeze-drying

In this technique,[55] water is added to a polymer solution to form an emulsion. The polymer/water mixture is cast into a mold and quenched using liquid nitrogen. The scaffold is then freeze-dried to remove the dispersed water and solvent. The porosity and pore size is dependent on parameters such as the ratio of polymer solution to water, and emulsion viscosity. Scaffolds with porosities of up to 95% and median pore sizes between 13 to 35 μm have been prepared using this technique.[55] This method is limited by the small pore sizes obtained as well as the sensitivity of process variations.

2.3.3.5 Solvent Casting/Particulate Leaching (SCPL)

One of the most common scaffold fabrication methods is the solvent casting and particulate leaching technique. In this technique, porogen particles are used to generate pores. The particles are packed into a predesigned mold and a polymer solution is cast over the particle assembly. Following solvent evaporation, the porogen particles are removed through leaching, leaving a porous structure. When selecting the porogen/polymer/solvent combination, careful consideration should be taken. First, the porogen should not be soluble in the solvent used to dissolve the polymer, and second, the polymer should not be soluble in the solvent used to leach the porogen.

The first porogens used in this technique were salts such as sodium chloride, sodium tartrate, and sodium citrate.[56] Although salts such as sodium chloride and ammonium chloride[18] are still the most commonly used porogens because they are readily available and easy to handle, the use of other types of porogens has also been investigated. In particular, researchers have investigated the use of spherical porogens because they can be closely packed together, which results in more interconnection between the resulting pores formed following leaching. As such, paraffin spheres have been prepared for use as a porogen with promising results.[57,58,18, 59] For example, highly open and interconnected polyurethane scaffolds with an average porosity of 84% were fabricated using paraffin spheres.[18] Another group compared the morphology of scaffolds prepared using three different porogens: sodium chloride particles, paraffin spheres, and gelatin spheres.[43] They found that the scaffolds prepared with spherical porogens showed better mechanical performance and lower flow resistance.[43] The use of gelatin spheres as a porogen has shown promise due to its biocompatibility and potential to be used with a wide range of polymers.[60,61,62] Gelatin is known as a material that enhances cell attachment and proliferation.[63] A comparative study on the biocompatibility of scaffolds prepared using gelatin porogens and salt porogens showed that scaffolds made with gelatin porogens enhanced cell attachment.[63] However, one drawback of using gelatin as a porogen that has been reported is that it is difficult to achieve high scaffold porosity since high weight fractions of gelatin led to swelling during leaching.[64]

Sugar particles,[41] cubes,[65] spheres,[66,67] and fibers[41] have also been used as porogens in the particulate leaching technique and are reported to be good choices due to their biocompatibility and ease of use. In one approach, sugar spheres were prepared by spheronizing sugar particles using a horizontal Meker-Fisher burner flame.[68] Scaffolds fabricated using sugar spheres as a porogen were highly porous with interconnected pores. Rabbit bone marrow mesenchymal stem cells were found to adhere to the scaffold and proliferate *in vitro* over 21 days.[68] Another group has investigated the use of alginate beads as a porogen.[69] The beads were prepared by an emulsification and ionic gelation technique, whereby the size and shape of the beads could be controlled by altering process conditions. ATR–FT-IR spectroscopy demonstrated the existence of alginate molecules on the surface of the PLA scaffold fabricated using the alginate beads, which was shown to significantly enhance osteoblast adhesion and proliferation.[69]

Polyethylene glycol (PEG) has also been reported for use as a porogen in the particulate leaching technique.[70] PEG is biocompatible and the resulting scaffolds showed excellent morphology in terms of interconnection between the pores.[70] However, use of this porogen extended the time required for scaffold fabrication due to the extra time required to leach the PEG.[70]

In general, the main advantage of the solvent casting/particulate leaching technique for scaffold fabrication is that the porosity and pore size can be easily controlled. The amount of porogen added relates to the porosity, while the size of the porogen

particles is directly related to the size of the pores in the resulting scaffold. However, one difficulty that is often faced when using this technique, particularly for scaffolds requiring lower porosity levels, is the lack of interconnection between pores. This is because the spatial organization of the resulting scaffold is directly related to the spatial arrangement of the porogen particles in the porogen/polymer composite.[52] If the volume fraction of porogen particles is decreased, the number of contact points between particles decreases, and thus the interconnection between the pores formed after leaching also decreases. If the volume fraction of porogen particles is typically less than 65% for rigid spheres, a completely open-celled structure cannot be obtained due to the isolated particles in the polymer matrix.[71,72] Furthermore, with this scaffold fabrication technique, the interconnection between the pores is smaller than the size of the pores, which may limit the propagation of cells from one pore to another in certain applications.[52]

In view of these difficulties, studies have been conducted to improve pore interconnectivity when using the particulate leaching technique. For example, pretreatment has been imparted to partially bond the porogen particles by working in a humid environment in the case of NaCl porogen or by heat treatment in the case of paraffin spheres or sugar particles.[73,66,58] Interconnectivity has also been improved by utilizing a pressure differential/particulate leaching technique.[18] In this method, porogen particles are packed into a cylindrical mold where an air supply is connected to the top of the mold and a vacuum is connected to the bottom. Due to the pressure differential created, the particles are more tightly packed, which results in improved

interconnection between pores in the resulting scaffold. This method is also advantageous because the air-scaffold interface is eliminated by using a closed chamber. This prevents skin formation and ill-defined pore structures at the surface, which are common problems faced when using the solvent casting/particulate leaching method.[18]

In order to eliminate the need for organic solvents, which can potentially be harmful to cells, it was proposed that the solvent casting step in SCPL be replaced by melt-molding, resulting in the melt-molding/particulate leaching method.[74] In the melt-molding step, polymer powder and porogen particles are premixed and then hot-pressed together.[74] Although this eliminates the need for organic solvents, the elevated temperatures make it difficult to include cells or bioactive molecules during processing.

Another drawback of the solvent casting/particulate leaching technique is the limitations on scaffold thickness. Preparation of thick foams using this technique is not practical because of the time required for the casting and leaching steps. However, for applications that do not require exceptionally large foams, such vascular tissue engineering, this is not an issue.

2.3.3.6 Rapid prototyping/solid free-form fabrication

Rapid prototyping (RP) or solid free-form (SFF) fabrication refers to a group of techniques that model a scaffold directly from a computer-aided design (CAD) data

set.[75] Examples of these techniques include 3D-printing, selective laser sintering, 3D-plotting, and fused deposition modeling.[76] RP techniques build up a specific body shape by the selective addition of material, layer-by-layer, guided by a computer program.[75] The advantage of these techniques it that complex scaffolds with an exact predefined shape can be fabricated.[75] However, these techniques are time consuming and are limited to pore sizes greater than 50 μm and porosities lower than 70%.[52]

2.3.3.7 Combined Techniques

It is often beneficial to use a combination of different scaffold fabrication techniques and it also offers more flexibility. For example, in a combination of gas foaming and particulate leaching,[77,78] ammonium bicarbonate was added to a polymer solution in methylene chloride or chloroform, forming a highly viscous mixture that can be shaped with a mold. After solvent evaporation, the composite is immersed in warm water, which results in concurrent gas evolution and particle leaching. This method greatly improved the pore interconnection of the gas foaming technique and porosities of up 90% were obtained.[77]

The particulate leaching technique has also been combined with the phase separating,[54] emulsification/freeze-drying,[55] and rapid prototyping techniques.[79] These combined techniques result in the creation of a multi-porous structure characterized by different pore sizes and/or pore morphologies. However, control over scaffold morphology is difficult.

2.3.3.8 Electrospinning

Electrospinning is a polymer-processing technology used for the production of polymer fibers. Polymer fibers with diameters from 3 nm to greater than 5 μm have been produced with this technique.[80] The technology of electrospinning first appeared in the 1930s, but the technique has only recently gained interest within the tissue engineering community as a means to fabricate scaffolds.[40]

A typical electrospinning setup consists of a syringe pump, a high voltage source, and a collector. In the electrospinning process, the electric field created by the high voltage source is used to draw polymer solution or melt through the needle to the collector. The application of an electric field induces charges within the polymer, resulting in charge repulsion within the solution.[81] Eventually, this charge repulsion overcomes the surface tension and a fine jet is ejected from the needle. The solvent in the ejected jet begins to evaporate to form polymer fibers that travel toward the grounded counter electrode where they are collected.

The electrospinning process can be manipulated to achieve the desired fiber diameter and morphology of the resulting fiber mesh. For example, when electrospinning polyurethaneurea solutions, fiber diameters in the range of 7 nm to 1.5 μm were obtained by varying the solution concentration.[82] Tunable parameters include: polymer solution concentration, solution feed flowrate, distance between the needle tip and collector, and applied voltage.

One of the drawbacks of the electrospinning technique is that nonwoven sheets with a two-dimensional profile are usually produced because it is time-consuming to produce thicker 3D meshes due to the low flowrate required.[40]

Modifications to the electrospinning technique have been developed to suit specific applications. One such development is a multi-layering electrospinning technique designed for fabrication of scaffolds for blood vessel tissue engineering.[83] In the multi-layering technique, a rotating mandrel-type collector is used to produce aligned nanofiber matrixes. Aligned nanofibers can be advantageous because cell orientation can be controlled.

Electrospinning is the most appealing method for producing nanoscaled polymeric fibers because it is the most simple and efficient.[40] It also shows promise as a scaffold fabrication technique because it offers the ability to fabricate scaffolds that closely mimic the scale and fibrous nature of the native ECM.

2.4 Specific Objectives and Rationale

Isolated cells need a specific environment to guide their growth for new tissue formation, and tissue engineering scaffolds play a significant role in creating such an environment. The success of tissue regeneration greatly depends on the microstructure and morphology of this supporting structure. These properties are of course governed by the fabrication technique. The focus of this work was to fabricate scaffolds for vascular tissue engineering applications from biostable polyurethane.

The rationale for choosing biostable polyurethane is based on previous investigations by our laboratory for vascular tissue engineering.[16, 18, 84-86] The specific objectives were as follows:

- Prepare alginate beads that are suitable for use as a porogen.
- Fabricate highly porous 3D polyurethane scaffolds by SCPL and electrospinning.
- Evaluate and compare their fabrication-method dependent morphology.
- Study the interaction of vascular smooth muscle cells with these scaffolds.

CHAPTER 3

3 Materials and Methods

3.1 Materials

Poly(carbonate urethane) (PCU) (Bionate® 55D) was supplied by the Polymer Technology Group (Berkeley, CA) and was used as the scaffold material in this work. Sodium Alginate (Manucol® LKX) was obtained from ISP Pharmaceuticals (Wayne, NJ). Gelatin microspheres (120-150 μm) were purchased from Thies Microcapsules™ (Henderson, NV). D-fructose, ethanol, Dimethylformamide (DMF), Dimethylsulfoxide (DMSO), Ethylenediaminetetraacetic acid (EDTA), Span® 80 (Sorbitane monooleate), Tween® 80 (Polyethylene glycol sorbitan monooleate), mineral oil, isooctane, hexane, and calcium chloride were purchased from Sigma Aldrich. Human coronary artery smooth muscle cells (HCASMCs), and smooth muscle growth medium-2 bullet kit (SmGM-2) were purchased from Lonza Walkersville Inc. (Walkersville, MD). Fibronectin was purchased from Santa Cruz Biotechnology (Santa Cruz, CA). Paraformaldehyde was purchased from EMD Chemicals (Gibbstown, NJ). Alexa Fluor® 568 phalloidin, and 4',6-diamidino-2-phenylindole (DAPI) were purchased from Invitrogen (Eugene, OR). SHUR/Mount™ Liquid Mounting Medium was obtained from Triangle Biomedical Sciences Inc. (Durham, NC).

3.2 Methods

3.2.1 Alginate Bead Preparation

Alginate beads were prepared by an emulsification and ionic gelation technique as previously reported[69,87] with notable modifications. 50 mL of 4.5 wt% aqueous sodium alginate (1, 2, and 3 wt% were used in preliminary experiments) was added drop-wise to a 250 mL beaker containing 75 mL of mineral oil (isooctane was used in preliminary experiments) with 1.2 mL of Span® 80 while mixing at 300 rpm using an overhead mixer. After mixing for 10 minutes, 5 mL of deionized water containing 0.7 mL Tween® 80 was added. Following mixing for another 20 minutes, 30 mL of calcium chloride solution (of varying concentration: 100, 150, and 200 mg/mL) was added. In order to allow the ionic cross-linking to go to completion, the emulsion was left mixing overnight. The beads were then filtered, washed with hexane, and allowed to dry at ambient temperature in a fume hood for at least 30 minutes. The beads used as a porogen for scaffold fabrication were finally sieved to a particle size range of 106-300 μm. Scanning electron microscope (SEM) images of the beads were captured using the procedure described in Section 3.2.3.1. For each experiment, a total of 100 particles were selected and their bead diameters were measured using ImageJ software (NIH, Bethesda, MD, USA). Data were then analyzed using two-tailed, unpaired Student's t-tests for n=100, and statistical significance was assigned for $p < 0.05$.

3.2.2 Scaffold Fabrication

3.2.2.1 Solvent casting/particulate leaching

A pressure differential solvent casting-particulate leaching method (SCPL)[18] was used to fabricate scaffolds using one of three different types of porogen particles: alginate beads (sieved to 106-300 μm), gelatin microspheres (120-150 μm), and D-fructose particles (sieved to 180-212 μm). In each case, the respective porogen particles were first packed into a cylindrical mold (5.5 mm diameter, 8 cm height). This was done by subjecting the particles to a pressure differential after incremental amounts were added. The pressure differential was created through a nozzle at the top, which supplied air, and a nozzle at the bottom, which applied a vacuum (see Figure 1). Once the column was packed, a viscous solution of PCU (25% v/v) dissolved in DMF was added to the top of the porogen bed and forced through the entire packed column using an air supply line and vacuum. Note that in the case of the scaffolds fabricated using D-fructose as a porogen, a solvent mixture of DMF and DMSO (with various mixture ratios) was used to dissolve PCU whereas in the case of the scaffolds fabricated using alginate or gelatin as a porogen only DMF was used. Once the polymer solution had infiltrated through the porogen assembly, the mold was removed from the apparatus and the cylindrical construct was pushed out of the mold using a metal rod. With the exception of scaffolds fabricated using gelatin porogens and the combined SCPL/Phase inversion (PI) method, scaffolds were then placed in a fume hood for 3 days to allow the solvent to evaporate. Scaffolds fabricated using gelatin and combined SCPL/PI were immersed in 95% ethanol before the leaching step. The porogen particles were then leached out by submerging in deionized water

at room temperature (in the case of fructose) or at 60°C (in the case of gelatin) or by immersing in 0.1 M EDTA at 35°C (in the case of alginate). Scaffolds were leached for 2 days (fructose porogen) or 4 days (gelatin and alginate) while exchanging the leaching solvent every 12 hours. Scaffolds immersed in EDTA required an additional step and had to be immersed in water for another day to remove residual EDTA.

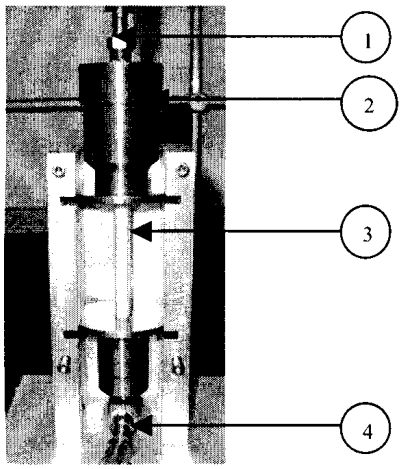

1. Air supply
2. Stainless steel body
3. Glass cylindrical mold (5.5 mm diameter and 8 cm height) containing porogen particles
4. Vacuum application

Figure 1: Apparatus used for fabrication of scaffolds by SCPL

3.2.2.2 Electrospinning

Various concentrations (5, 10, 12.5, 15% v/v) of PCU in DMF were prepared. The solution was transferred to a plastic syringe equipped with a stainless steel needle (22 gauge needle, OD=0.7176 mm, ID=0.413 mm), which was connected to a high voltage supply (set at 15 kV, 18 kV, and 20 kV). The solution was fed through the needle using a syringe pump (set at a flowrate of 0.1 mL/h or 0.15 mL/h), and the grounded collector was located 8 cm from the tip of the needle.

3.2.3 Scaffold Characterization

3.2.3.1 Scanning Electron Microscopy (SEM)

Scaffold morphology was visualized using Scanning Electron Microscopy (SEM). Samples were first mounted on carbon-taped aluminum stubs and gold sputtered (Emitech K550X) with a current of 15 mA and a run time of 1.30 minutes. The stub was then placed in the SEM (S- 2600N, Hitachi, Japan), where the sample was subjected to a vacuum and the tungsten filament was turned on. The secondary electron detector was used and the voltage for the electron beam was set to 5 kV. The imaging could then be performed at various magnifications. From SEM images, scaffold pore size and fiber diameter were measured using ImageJ software (NIH, Bethesda, MD, USA). A minimum of four SEM micrographs was selected for measurements and data were analyzed using two-tailed, unpaired Student's t-tests. Statistical significance was assumed for $P<0.05$.

3.2.3.2 Microcomputed tomography (MicroCT)

Samples were imaged by microcomputed tomography (microCT) (GE Locus, GE Healthcare, Canada). Scans were preformed with an x-ray voltage of 80 kV and a current of 0.45 mA, and reconstructed at an isotropic voxel size of 0.020 mm. 2D slice images were reconstructed and compiled to generate a 3D image, and the images were analyzed using a commercially available trabecular bone analysis software (MicroView, GE Healthcare). Porosity, pore size, strut thickness, and surface-area-to-volume ratio measurements were analyzed using two-tailed, unpaired Student's t-test (statistical significance assumed for $p<0.05$).

3.2.3.3 Mercury Porosimetry

Measurements were made using an Autopore IV porosimetery (Micromeritics, Norcross, GA). Cylindrical scaffold samples were cut into disks having a mass between 0.015 and 0.03 g before placing in the penetrometer. The filling pressure of the penetrometer was 0.5 psi and the maximum pressure was 60 psi. Data analysis was carried out using the Washburn equation, which relates pressure to the size of the intruded pore diameter[88]: $DP = -4\gamma\cos\theta$, where D represents pore diameter, P is applied pressure, γ is surface tension, and θ is the contact angle between mercury and pore wall. The surface tension of mercury and the intrinsic contact angle with the scaffolds were taken to be γ_{Hg} = 485 dynes/cm and θ = 130° respectively. Scaffold porosity was calculated from the total intrusion volume, polymer density, and sample mass.

3.2.4 Cell Proliferation and Cytotoxicity

In preparation for cell culture studies, scaffolds prepared by SCPL were sliced into ~1 mm cylindrical disks using a rotating razor blade while electrospun mats were cut into cylindrical disks having a diameter of 12 mm. All samples were affixed to a 24-well cell culture plate (BD Falcon™, Franklin Lakes, NJ) using silicone grease, sterilized by immersion in 70% ethanol for 30 min, and allowed to dry for 30 min under germicidal UV light. Samples were then coated with fibronectin (5 μg/sample) for 1 hour at room temperature according to the supplier's instructions.

Human coronary artery smooth muscle cells (HCASMCs) between passage 5 and 8

were used for cell culture studies. HCASMCs were cultured in SmGM-2 supplemented with 1% penicillin/streptomycin solution (P/S). Cultures were maintained in a humidified incubator at 37°C and 5% CO_2. HCASMCs were seeded onto samples at an initial cell density of approximately 50×10^4 cells/sample and cultured for 7 and 14 days before fixation and immunostaining. Following culture time, cells were fixed for 20 min at room temperature in 4% paraformaldehyde in divalent cation-free PBS and permeabilized with 0.5% Triton X-100 in PBS. HCASMCs were incubated for 1 hour at ambient temperature in 1% BSA/PBS containing Alexa Fluor® 568 phalloidin (1:50 dilution). DAPI (300 nM in PBS) was used to label nuclei. Samples were mounted on slides in SHUR/Mount™ and analyzed with a Zeiss LSM 410 confocal microscope (Carl Zeiss, Toronto, ON, Canada) equipped with an argon/neon as well as a UV laser.

For cytotoxicity, 3-(4,5-dimethylthiazol-2-yl)-2,5-diphenyltetrazolium bromide (MTT) assay was carried out following the manufacturer's protocol (Vybrant®, Invitrogen, Burlington, ON, Canada). The initial cell density was 6×10^4 cells/scaffold in 96-well tissue culture plates which were then cultured for 7 and 14 days. An MTT solution was added to each well to make the final concentration 1.10 mM and then incubated at 37°C. After removal of the supernatant, 10% (weight/volume) SDS was added and the absorbance was recorded at 570 nm by a plate reader. Negative control experiments were carried out by adding MTT to the culture medium only.

CHAPTER 4

4 Results and Discussion

4.1 Scaffold Material Selection

Biodegradable scaffolds are often preferable as a responsive tissue *de void* of scaffold fragments is the ideal alternative when compared with hybrid constructs;[16] but they have a number of disadvantages. Commonly used biodegradable polymers such as poly(L-lactic acid), poly(glycolic acid), and their copolymers often generate acidic degradation products, and this raises concerns that the scaffold microenvironment may not be ideal for tissue growth.[70, 84] In addition, strict coordination of scaffold biodegradation and extracellular matrix deposition is required.[39] The tissue maturation process is also generally lengthy, especially in vascular tissue engineering applications, since vascular tissues have to be mechanically strong and function immediately upon implantation.[84] For these reasons, considerable attention has recently been given toward the use of nondegradable scaffolds in vascular tissue engineering.[16, 89, 90] Polyurethanes have shown promise as a scaffold material in the design of hybrid vascular substitutes due to their proven mechanical properties.[16, 18, 84] Furthermore, in order to effectively study the influence of scaffold morphology on cellular interactions, biostable scaffolds are preferable, since scaffold degradation is linked to scaffold morphological characteristics. Thus, biostable poly(carbonate urethane) (PCU) (Bionate® 55D) was selected as the scaffold material in this work.

4.2 Alginate Beads as a Porogen

Alginates are generally regarded as non-toxic and biocompatible and are widely used in the pharmaceutical, cosmetics, and food industries.[91] This makes them a good choice for use as a porogen, since residual alginate would not be cytotoxic. Although the use of alginate particles to fabricate poly(D,L-lactic acid) (PLA) scaffolds for bone tissue engineering applications has been reported,[69] the bead sizes and the resulting pore sizes were too large for vascular tissue engineering applications and scaffold morphology was not extensively studied.

4.2.1 Porogen Bead Preparation and Stability

Alginate (or alginic acid) is a naturally occurring hydrophilic colloidal polysaccharide isolated from brown seaweed (Phaeophyceae). It is a linear polymer composed of β-D-mannuronic acid (M) and α-L-guluronic acid (G) residues arranged in the polymer chain in blocks (see Figure 2). These homogeneous blocks are separated by blocks made of random or alternating units of mannuronic and guluronic acids.[91] The relative amount of these blocks varies with the source of the alginate.

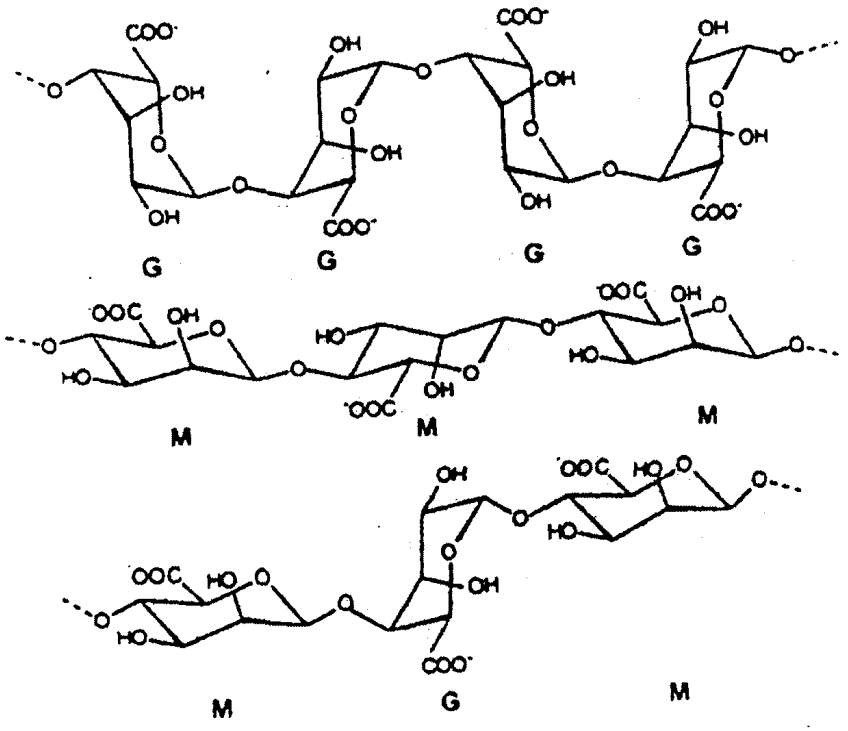

Figure 2: Different alginate block types. G = guluronic acid, M = mannuronic acid.[91]

Alginates have the ability to form two types of gels. At low pH (below 4), hydration of alginic acid leads to the formation of a high-viscosity 'acid gel,' while at a pH above 4, monovalent metal ions can form soluble salts with alginate, and cross-linking with divalent cations such as Ca^{2+}, Zn^{2+} and Cu^{2+} leads to ionotropic gelation.[87, 91] In the latter gelation technique, the divalent cation replaces the monovalent Na cation and binds to the polymer wherever there are two neighboring guluronic acid residues, resulting in cross-linking of both different polymer molecules as well as different parts of the same chain.[92] This technique is often used for microencapsulation of drugs, proteins, cells, and DNA.[87]

The most common method for preparing alginate microspheres is by extruding sodium alginate solution as droplets into calcium chloride solution.[87] However, this method typically produces beads with a diameter greater than 1 mm.[93] Given that the optimal pore size range for scaffolds for vascular tissue engineering applications has been reported as 100-300 microns,[16, 89] the extrusion technique is not suitable for preparing beads for use as a porogen in this study. Instead, alginate beads were prepared by an emulsification technique, which is more appropriate for producing smaller sized microspheres.[94] In this method, aqueous sodium alginate solution is dispersed in an immiscible organic phase to which calcium chloride solution is then added.

The formation of beads by emulsification is thermodynamically unfavorable and requires a greater degree of chaos than does the extrusion method. The extrusion method relies only on simple diffusion for gelation of alginate to take place, while the emulsification method is more complicated due to the presence of an organic phase and the need for dispersion stability to prevent aggregation of dispersed alginate globules.[87] For this reason, the use of two surfactants was required. Span® 80 (Sorbitane monooleate) and Tween® 80 (Polyethylene glycol sorbitan monooleate), two nonionic surfactants, were chosen based on their solubility, Hydrophile Lipophile Balance (HLB), as well as previous work that reported the use of these surfactants in the formation of alginate beads.[69]

There are many process parameters that affect the emulsion stability as well as the resulting bead size and shape. These include surfactant concentration, sodium alginate concentration, calcium chloride concentration, type of oil used, and mixing speed.

At the early stage of this study, preliminary experiments were carried out using isooctane, which has been used extensively as the lipophilic phase in previously reported studies.[69,87,94,95] However, problems with emulsion stability were encountered. The sensitivity of the process to slight process variations resulted in notable batch-to-batch variations making it difficult to produce reliable data. Furthermore, the beads tended to agglomerate to one another following the drying step. This can be seen in Figure 3, where SEM images of alginate beads prepared using isooctane and three different sodium alginate concentrations (1, 2, and 3 wt%) are shown. Alterations to surfactant concentration and calcium chloride concentration were carried out, but these alterations did not result in notable improvements in terms of bead agglomeration or morphology, nor were there quantifiable changes in bead size (data not shown). However, bead diameter was observed to increase with increasing sodium alginate concentration, the beads having average diameters of 45.0 $\pm$ 15.7 μm, 175.2 $\pm$ 63.1 μm, and 228.8 $\pm$ 101.0 μm (expressed as mean $\pm$ standard deviation) with sodium alginate concentrations of 1, 2, and 3 wt% respectively (see Figures 3A-C).

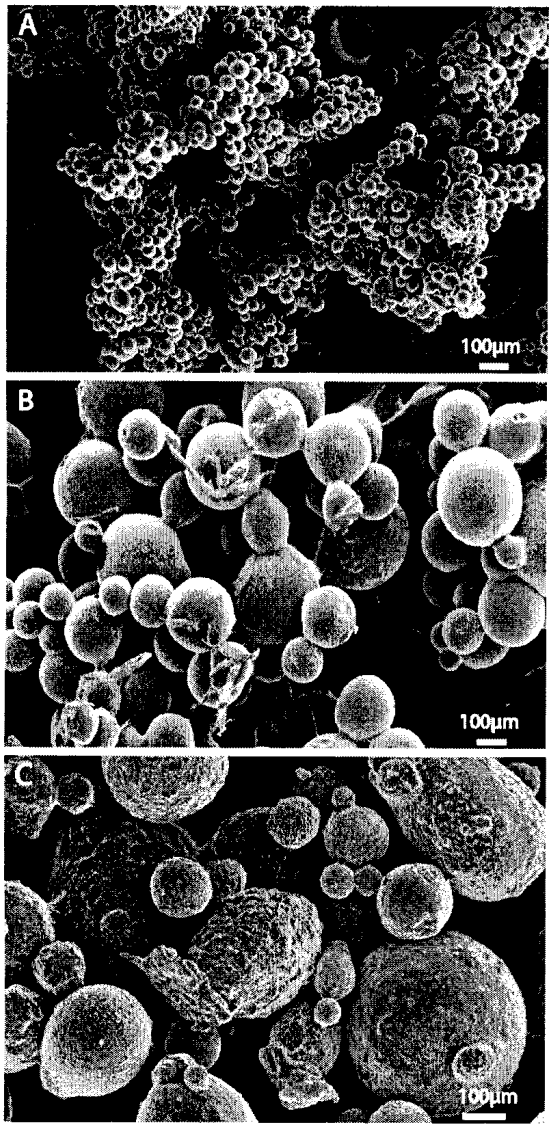

Figure 3: SEM images of alginate beads prepared using isooctane and a sodium alginate concentration of 1 wt% (A), 2 wt% (B), and 3 wt% (C). Note: all other parameters remained constant (1.2 mL Span® 80, 0.7 mL Tween® 80, 150 mg/mL $CaCl_2$).

An increase in sodium alginate concentration results in an increase in viscosity of the dispersed phase, which in turn increases the size of the emulsion droplets and decreases emulsion stability due to the higher energy level needed to disperse a solution of higher viscosity. The decreased stability also results in more irregularly shaped beads with a rougher surface (see Figure 3C).

In an effort to improve emulsion stability and avoid agglomeration of the beads, which has been reported to be a common problem encountered when preparing alginate beads using the emulsification technique,[96, 97] mineral oil was used as the lipophilic phase instead of isooctane. The rationale here is that the increase in oil viscosity reduces the diffusion coefficient of the dispersed droplets, which reduces their frequency of collision and rate of coalescence, and increases emulsion stability. Figure 4A shows a representative image of beads prepared using mineral oil as the lipophilic phase which supported this assumption. Minimal bead agglomeration was encountered, and the beads were more regularly shaped with a smoother surface. In addition, smaller beads were generally achieved when using mineral oil instead of isooctane. Furthermore, beads of the desired size range could be obtained at higher sodium alginate concentration, which made the process more efficient, since higher concentrations of sodium alginate produce larger quantities of beads in a single batch. When using mineral oil and a sodium alginate concentration of 4.5 wt%, beads with an average diameter of 145.3 $\pm$ 66.1 μm were obtained (Figure 4A). In contrast, when using isooctane and a sodium alginate concentration of 3 wt%, beads with a much larger average diameter (228.8 $\pm$ 101.0 μm), which was too large for the desired application, were obtained. In view of these advantages, mineral oil was found to be a better choice than isooctane and was used as the lipophilic phase for the remaining part of the study.

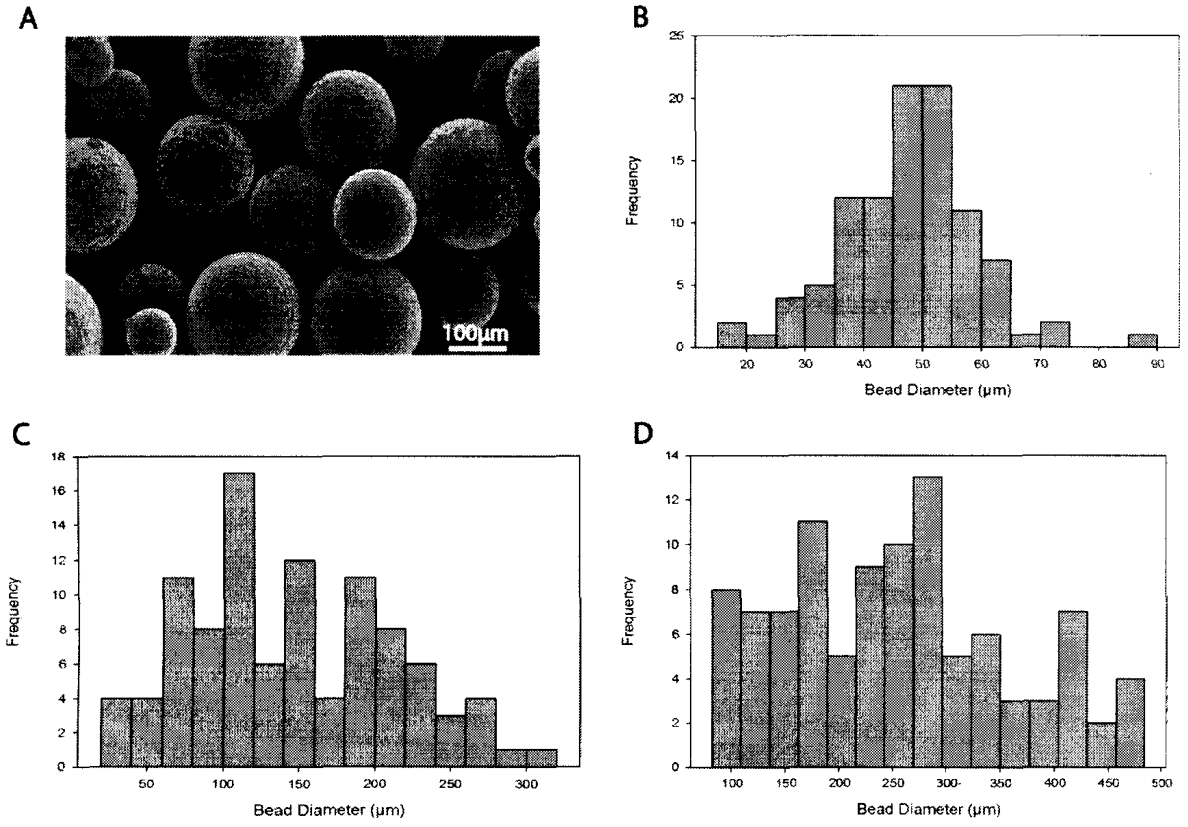

Figure 4: Alginate beads prepared using mineral oil, 4.5 wt% sodium alginate, 1.2 mL Span® 80, 0.7 mL Tween® 80, and 150 mg/mL $CaCl_2$ (A), and alginate bead size distribution (N=100) at a calcium chloride concentration of 100 mg/mL (B), 150 mg/mL (C), 200 mg/mL (D) (all other parameters are the same as in A).

Three different calcium chloride concentrations (100, 150, and 200 mg/mL) were evaluated in order to achieve the desired bead size. Past studies have shown that the mean size of microspheres is strongly related to the Ca^{2+} concentration.[69, 87] Figure 5 shows the effect of the calcium chloride concentration on the mean bead diameter. It can be seen that the bead diameter increases as the concentration of calcium chloride increases. This can be explained by examining the nature of the non-covalent ionic cross-linking. When the calcium chloride solution is added to the emulsion under constant mixing it is sheared into globules and the initiation of the ionic cross-linking is dependent on the chance collision between the alginate globules and the calcium

chloride globules. Upon collision, inter-globular or intra-globular cross-linking can occur.[87] Intra-globular cross-linking results in densification and size reduction, while inter-globular cross-linking causes alginate globules to combine and form a larger bead. The mean size of the beads formed depends on the net extent of inter-globular and intra-globular cross-linking. At higher calcium chloride concentration there is more Ca^{2+} available to exchange with Na^{+} and inter-globular cross-linking dominates, resulting in larger beads.

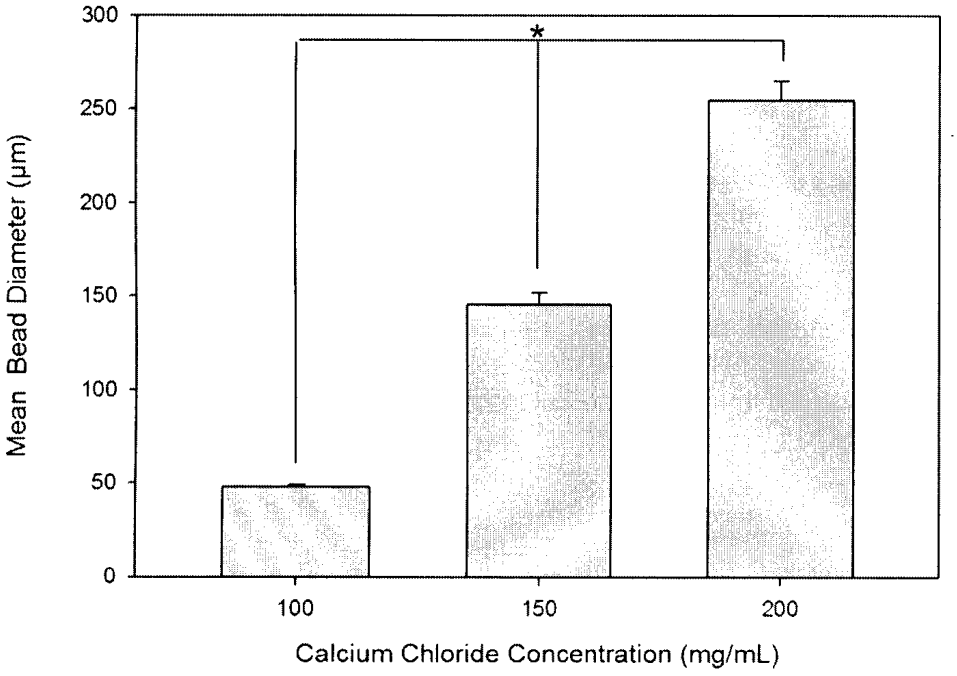

Figure 5: Effect of calcium chloride concentration on mean diameter of alginate beads. Error bars represent the standard error and * indicates statistical significance.

Figures 4B-D show that the bead-size distribution is also affected by the calcium chloride concentration. As the concentration increases the distribution widens

considerably. This makes sense because if the intra-globular cross-linking dominates such that the majority of the alginate globules do not combine to form larger microspheres, the resulting bead size should be similar to that of a single alginate globule in the emulsion with little variation. This was observed at a calcium chloride concentration of 100 mg/mL (Figure 4B). In contrast, as the concentration increased to 150 mg/mL, and then to 200 mg/mL, the size distribution widened considerably (Figures 4C & D).

In this study, the alginate beads that were prepared using a calcium chloride concentration of 150 mg/mL were selected for scaffold fabrication because the majority of beads were within the desired size range. Figure 4A shows an SEM image of the beads and it can be seen that they are spherical in shape. Spherical beads are preferred because they can be closely packed together during scaffold fabrication, which improves uniformity and interconnection of pores in the resulting scaffold.

4.3 Scaffolds Fabricated by SCPL

Solvent casting/particulate leaching is among the most versatile fabrication techniques, and the type and shape of porogen used play a major role in dictating the properties of the resulting scaffold. Thus, the use of three different types of porogens (alginate beads, D-fructose particles, and gelatin spheres) was evaluated. The results are discussed below.

4.3.1 Scaffolds Fabricated using Alginate Beads

Alginate beads sieved to a size range of 106-300 μm were used to fabricate scaffolds by the particulate leaching technique. The beads were leached out using 0.1 M EDTA, which is a calcium chelating agent.

Figure 6 shows the morphology of the resulting scaffold, from which it can be inferred that the pores are well interconnected and spherical in shape, owing to the shape of the alginate beads used.

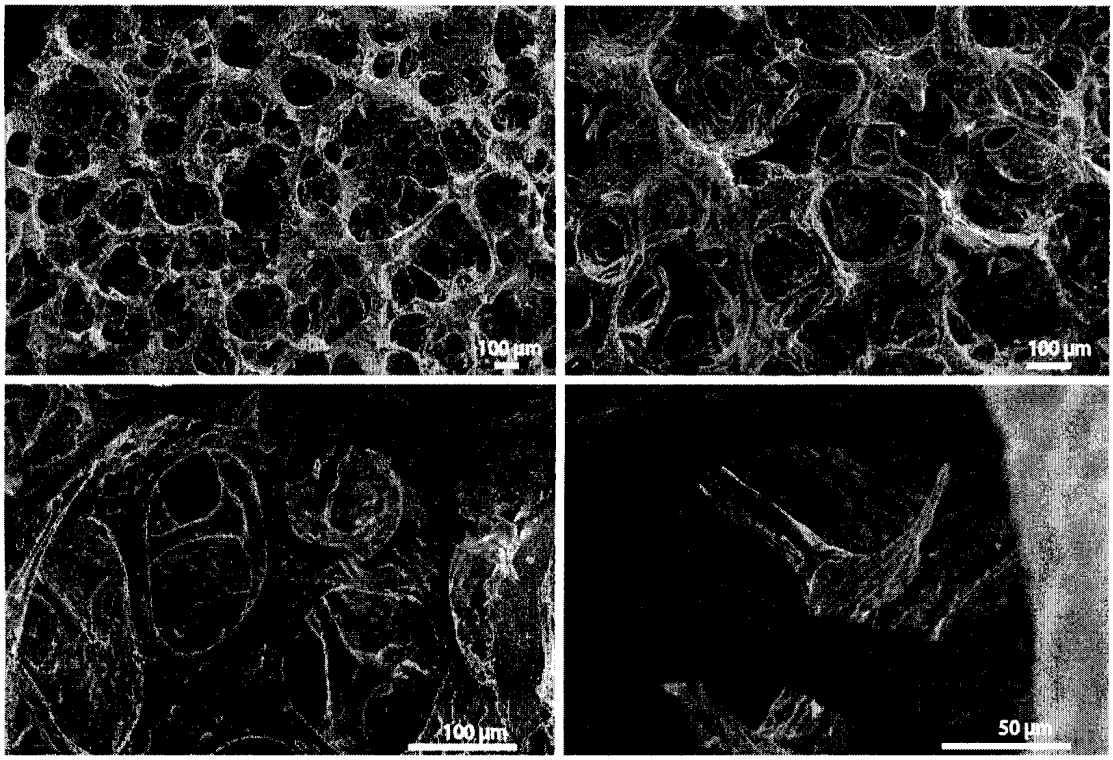

Figure 6: Representative SEM images of PCU scaffolds (different magnifications) fabricated by SCPL using alginate beads (106-300 μm) as a porogen.

As mentioned in Chapter 2, it is often difficult to obtain well-interconnected scaffolds with tailored pore shape, particularly when using the SCPL fabrication technique. One of the crucial points in scaffolding is the level of pore interconnection, since an open porous network is believed to enhance nutrient circulation, metabolic waste removal, and cell proliferation. Because of this, researchers have investigated incorporating additional steps, such as fusion of the porogen particles prior to solvent casting[73,66,58], in order to improve pore interconnectivity. Here, an interconnected pore network was achieved without any additional steps by using spherical alginate beads and employing a pressure differential solvent casting-particulate leaching technique, whereby the beads were tightly packed in a cylindrical mold using an air supply line (applied at the top) and vacuum (applied at the bottom).

In addition, the spherical pores obtained are advantageous because they allow for a more regular structure and uniform distribution of interconnections between pores. Studies have shown that scaffolds with spherical pores have lower flow resistance when compared with scaffolds with an irregular geometry of pores.[43] This in turn means improved fluid exchange and nutrient supply to cells.

MicroCT analysis was able to provide further insight into scaffold morphology. Figure 7A shows a 3D isosurface of a scaffold fabricated with alginate beads (lighter regions represent the polymer matrix while darker regions correspond to air), and Table 2 displays the quantitative results.

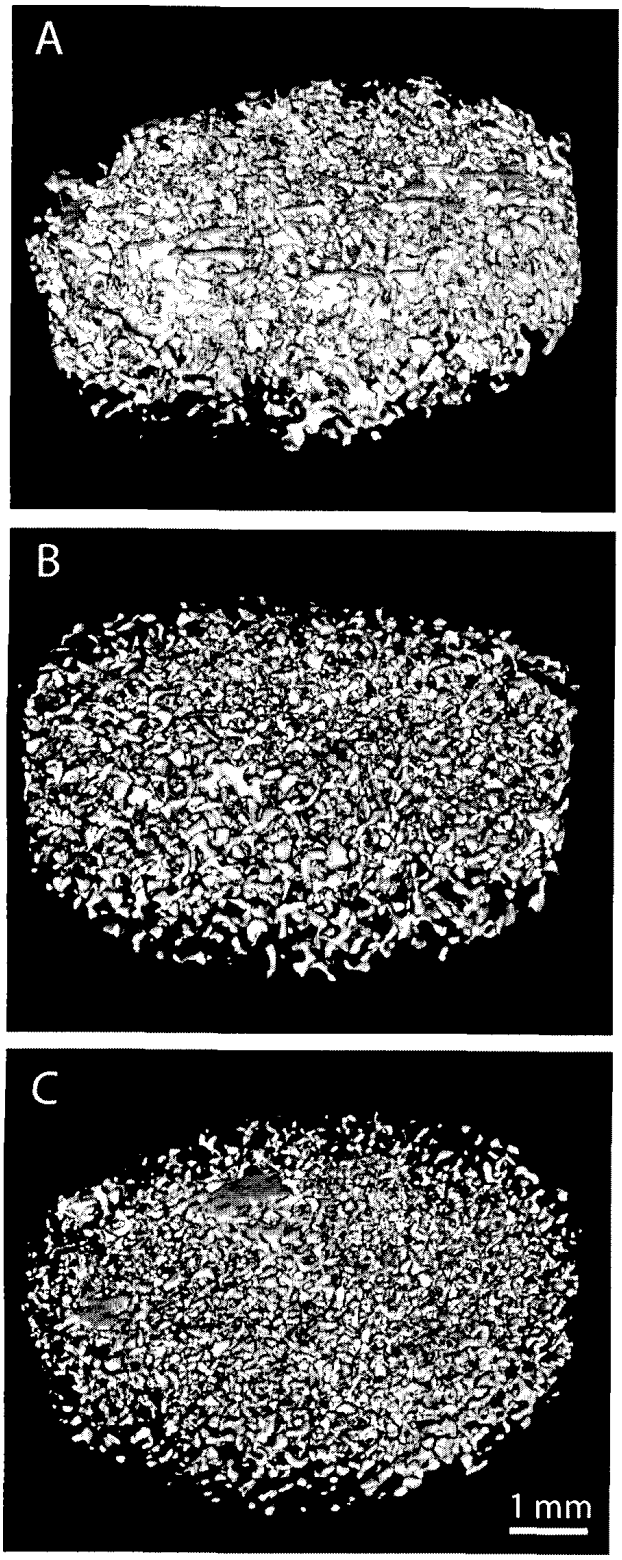

Figure 7: Representative MicroCT isosurfaces of PCU scaffolds fabricated by SCPL using alginate beads (A), D-fructose with a polymer solvent mixture of 30% DMSO/70% DMF (B), and D-fructose with polymer solvent mixture of 50% DMSO/50% DMF (C).

Table 2: MicroCT Analysis of PCU scaffolds fabricated using SCPL and two different types of porogens.

Porogen Type	Porosity (%)	Strut Thickness (μm)	Pore Diameter (μm)	Surface Area to Volume Ratio (mm^{-1})
Alginate	85.6 ± 4.5	29.1 ± 7.5	146.7 ± 34.3	84.7 ± 20.5
D-Fructose (30% DMSO)	88.1 ± 3.1	31.2 ± 6.1	172.1 ± 36.3	68.3 ± 11.3
D-Fructose (50% DMSO)	82.8 ± 7.5	27.3 ± 4.9	112.2 ± 33.2	86.5 ± 16.8

Data expressed as mean ± standard deviation for n = 27.
Analyzed using two-tailed unpaired Student's t-test ($p < 0.05$).

The average scaffold porosity was found to be 85.6%, which is within the optimal scaffold porosity range (80-90%) for vascular tissue engineering.[16, 89] An average surface-area-to-volume ratio of 84.7 mm^{-1} is also an attractive feature because it is toward the higher end of the range of values that have been reported as typical for the SCPL technique.[56, 98] A high surface-area-to-volume ratio is also a good indication of a well-interconnected scaffold morphology. The average strut thickness (29.1 μm) and average pore size (146.7 μm) were consistent with what was observed with SEM. The mean pore size was also consistent with the mean diameter of the beads used to fabricate the scaffold (refer to Figure 4C).

However, even after excluding the bead sizes above and below the range in which the beads were sieved prior to scaffold fabrication (beads were sieved to size range of 106-300 μm), the upper limit pore size (~181 μm) was noticeably less than the upper limit alginate bead size (~300 μm). This was most likely due to batch-to-batch variation in the preparation of the alginate beads, which resulted in slight shifts in the bead size distribution.

From Figure 5A it can be seen that although the scaffold morphology is fairly uniform throughout the 3D slice, slight variations in scaffold porosity exist. This is likely due to the tacky nature of the alginate beads, which causes them to adhere to one another as well as to the glass tube during scaffold fabrication. A potential solution to this problem that could be investigated in the future is to prepare the beads using an emulsification/internal gelation technique.[97, 99, 100] In this method, internal gelation can be achieved by adding an insoluble calcium salt to the sodium alginate solution. After formation of the emulsion, the internal gelation occurs by adding an oil-soluble acid that causes calcium ion release. This technique has been reported to improve emulsion stability and prevent the aggregation phenomenon.[97] The improved emulsion stability may also help to minimize batch-to-batch variations.

4.3.2 Scaffolds Fabricated using D-Fructose Particles

D-fructose is found in many foods and is a readily available and cost effective choice for use as a porogen. It is biocompatible and highly water-soluble, which means additional organic solvents are not needed to leach the fructose particles following

solvent casting. In this study, a novel method of tailoring scaffold morphology using D-fructose particles as a porogen was developed.

Typically, when using the SCPL method, the porogen particles should not be soluble in the solvent used to dissolve the polymer. However, in this study the effect of the partial solubility of fructose in the polymer solvent was evaluated. This was done by using a solvent mixture of DMF and DMSO to dissolve the polymer. The PCU used in this work is soluble in both these solvents while fructose is only sparingly soluble in DMF but is readily soluble in DMSO. The rationale here was that by altering the percentage of DMSO in the solvent mixture from 0-50% (v/v), scaffold properties such as pore size and shape could be controlled and that microporosity could be induced within the scaffold.

The D-fructose particles were sieved to a narrow size range of 180-212 μm to make it easier to observe the effects of altering the concentration of DMSO on the pore size in the resulting scaffolds. As can been seen in Figure 8, the fructose particles are irregularly shaped. It is important to note that since the particles are irregularly shaped and their aspect ratio differs from 1, there are likely to be particles that fall outside the sieve range.

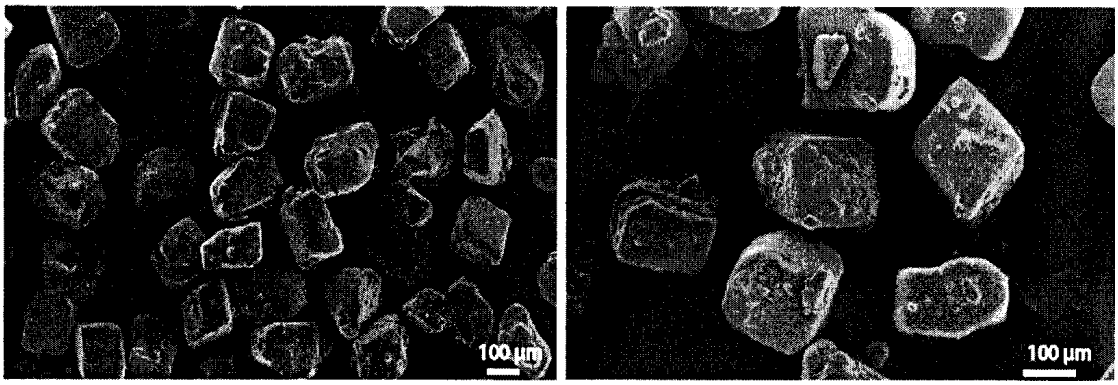

Figure 8: SEM images of D-Fructose particles (180-212 µm).

Figure 9 shows SEM images of scaffolds fabricated using different concentrations of DMSO in the polymer solvent mixture. Starting with just pure DMF as the polymer solvent (Figure 9A), it can be seen that the pores are well interconnected but irregularly shaped, which was expected due to the irregular shape of the fructose particles used. When a small amount of DMSO was added to make a polymer solvent mixture of 10% DMSO and 90% DMF, no noticeable changes to scaffold morphology were observed (Figure 9B). However, as the DMSO concentration in the polymer solvent mixture was gradually increased from 10 to 20, 30, 40 and 50% (Figures 9C-F), notable changes to scaffold morphology were observed. Pore size decreased and pore shape became more spherical as the concentration of DMSO increased.

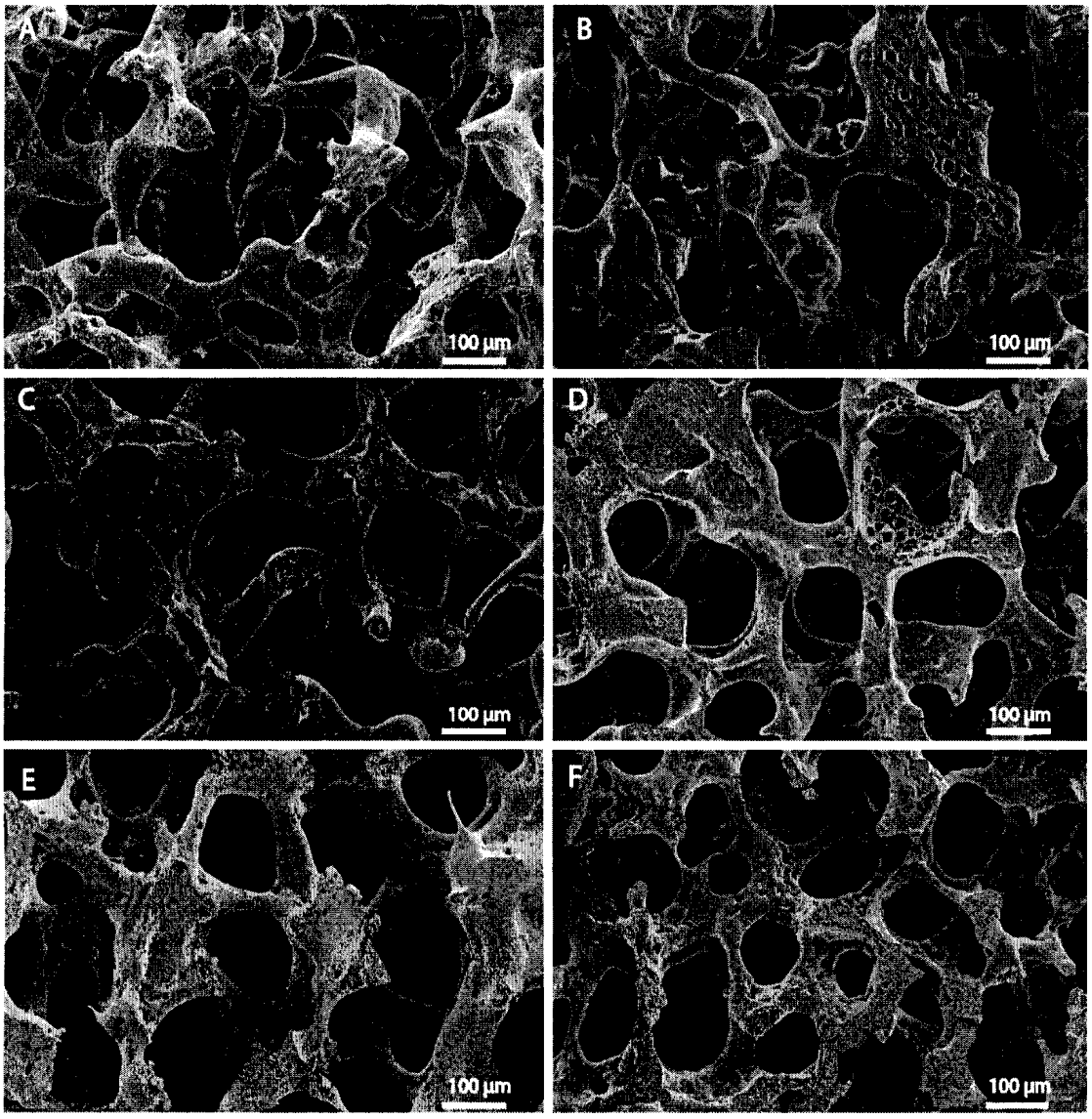

Figure 9: PCU scaffolds fabricated by SCPL using D-fructose as a porogen and various DMSO/DMF polymer solvent mixtures: 0% DMSO (A), 10% DMSO (B), 20% DMSO (C), 30% DMSO (D), 40% DMSO (E), 50% DMSO (F).

This was caused by the partial dissolution of fructose in DMSO prior to solvent evaporation. As fructose molecules began to break away from the surface of the particles and were transported into the solvent, the porogen particles became more spherical in shape in order to minimize surface tension. This resulted in scaffolds with

a more organized pore architecture, which is beneficial for nutrient supply and waste removal of cell metabolism.[31]

Figure 10 shows the effect of DMSO concentration on the mean pore diameter of PCU scaffolds. There was no significant difference in mean pore diameter for scaffolds fabricated with DMSO concentrations between 0 and 30%, but when increased from 30 to 40%, and from 40 to 50%, a significant decrease in mean pore diameter was observed.

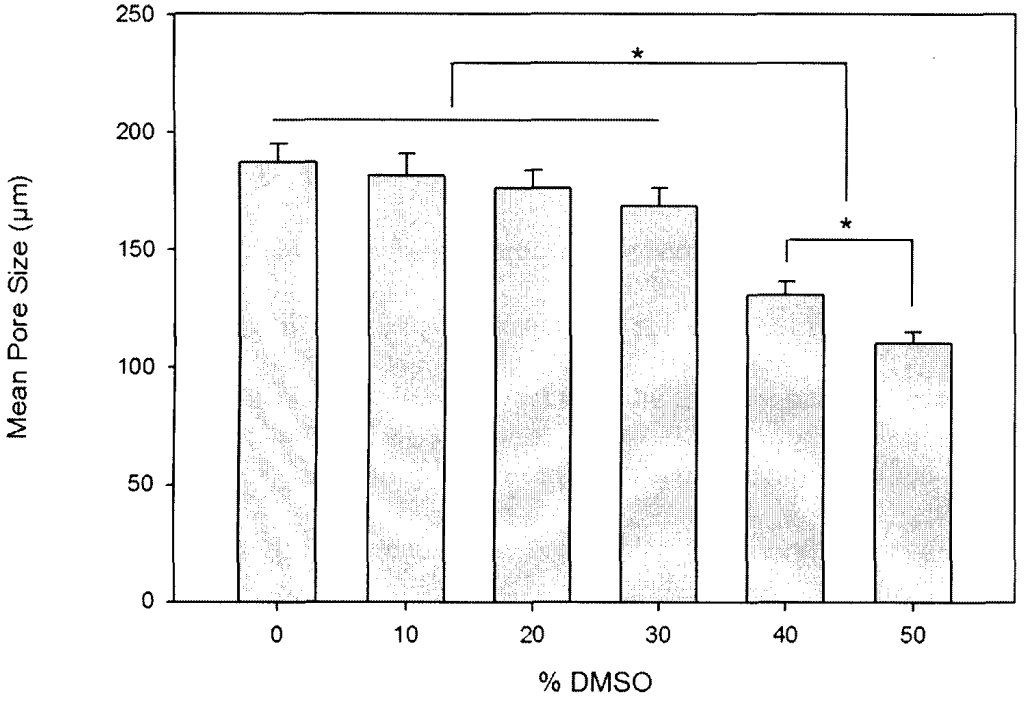

Figure 10: Effect of DMSO concentration on the mean pore diameter of scaffolds fabricated with D-fructose particles. Data expressed as mean ± standard error. Data connected with * are significant ($p<0.05$). Note: for each concentration, N=50.

MicroCT was used to conduct further analysis on the scaffolds fabricated using DMSO concentrations of 30 and 50% (refer to Figure 7 and Table 2). The results

were consistent with that of SEM analysis and showed a statistically significant decrease in mean pore diameter from 172.1 to 112.2 μm when DMSO concentration was increased from 30 to 50%. There was also a significant decrease in porosity from 88.1 to 82.8%. This was most likely caused by slight dissolution of the fructose particles during the solvent casting fabrication step for the higher DMSO concentration. At the higher DMSO concentration, where the polymer solvent mixture consisted of 50% DMSO and 50% DMF, problems with the uniformity of the scaffold were observed. MicroCT analysis showed that the porosity in the central regions of the scaffold slice was less than the outer regions, which resulted in a much larger standard deviation of 7.5% in contrast to only 3.1% for the scaffold fabricated using 30% DMSO. This observation could also be seen from the 3D representation of the scaffold slice (see Figure 7C). These less porous regions can be understood by looking at the solvent evaporation process. Solvent in the center regions of the cylindrical scaffold will take longer to evaporate since it must first diffuse through the construct. As a result, DMSO is in contact with the fructose particles in the center for a longer period of time than those in the outer regions. When the DMSO concentration is high, this causes a noticeable difference between the rate of dissolution of fructose in the center and that of the outer regions. This in turn causes a non-uniform distribution of pores throughout the scaffold when the DMSO concentration is at or above 50%.

In addition to the porosity and pore size, there was also a statistically significant difference in average strut thickness and surface-area-to-volume ratio between

scaffolds fabricated using 30% DMSO and those fabricated with 50% DMSO. Strut thickness is related to pore size, and for scaffolds with similar porosity, a decrease in pore size results in a decrease in average strut thickness since a larger number of pores must exist to maintain a constant porosity.[16, 88] Based on this reasoning, a decrease in pore size should also result in an increase in surface-area-to-volume ratio. Although there was a significant difference in the porosities of the two scaffolds fabricated with DMSO concentrations of 30 and 50% (Table 2), it did not invalidate these expected trends, since the p-value (0.0014) was much larger than the p-value calculated when comparing the average pore size (6.1×10^{-8}). At the higher DMSO concentration, the average strut thickness (27.3 μm) was significantly lower than at the lower DMSO concentration (31.2 μm). In addition, there was a significant increase in surface-area-to-volume ratio from 68.3 mm^{-1} (30% DMSO) to 86.5 mm^{-1} (50% DMSO). A high surface area is advantageous because it is believed to enhance cell attachment.[41, 98]

The effect of DMSO concentration on scaffold microporosity was also examined. Figure 11 shows a magnified view of the scaffold fabricated using 50% DMSO in order to show the micropores. From SEM analysis, microporosity appeared to increase with increasing DMSO concentration. Mercury porosimetry was carried out to examine this further, since MicroCT analysis was limited to a spatial resolution of 20 μm.

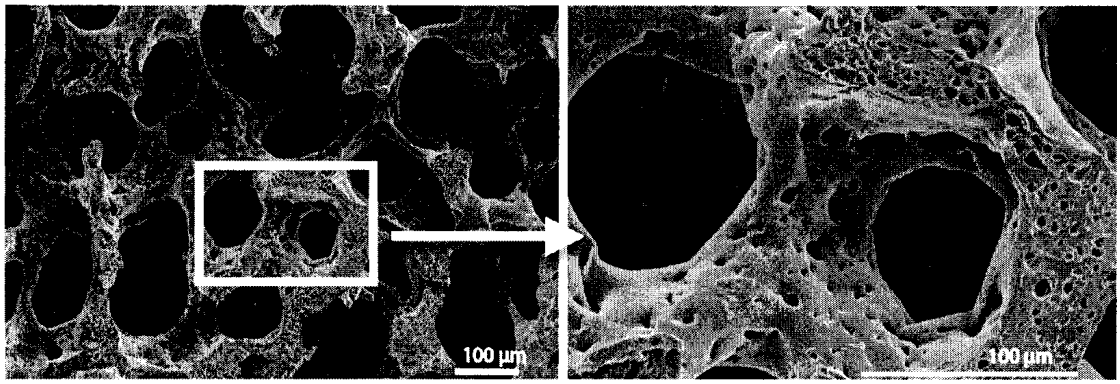

Figure 11: Microporosity of PCU scaffold fabricated by SCPL using D-fructose and a polymer solvent mixture of 50% DMSO and 50% DMF.

Figure 12 and Table 3 show the results of mercury porosimetry analysis conducted on scaffolds fabricated using 30 and 50% DMSO concentration. The peak pore diameter represents the pore diameter at which the largest fraction of mercury is intruded and corresponds to the maximum of the differential mercury intrusion profile.[101] The peak pore diameters were consistent with SEM and MicroCT analysis, since they were similar to the mean diameters found. In addition, as was found with MicroCT analysis, mercury porosimetry results showed that the porosity of scaffolds fabricated with 50% DMSO was lower than those fabricated with 30% DMSO. Although mercury porosimetry data presented scaffold porosities that were slightly lower than what was found with MicroCT, they were within an acceptable range, given the standard deviation calculated from MicroCT analysis.

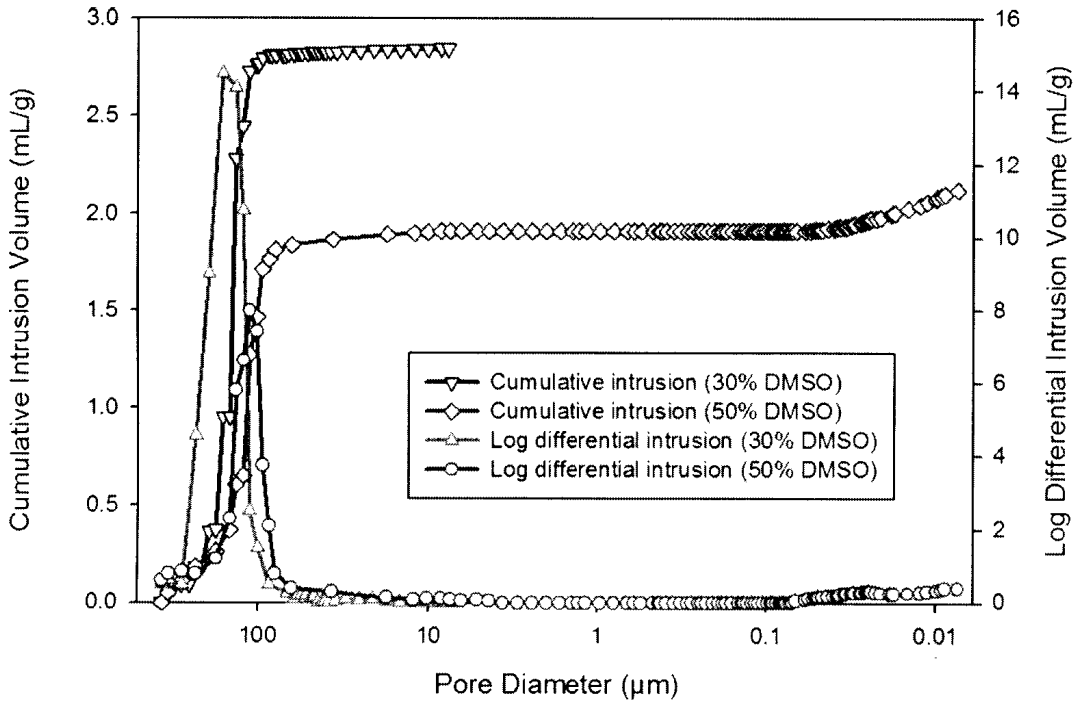

Figure 12: Mercury porosimetry results of PCU scaffolds fabricated by SCPL using D-fructose as a porogen and two different polymer solvent mixture concentrations: 30% DMSO/70% DMF and 50% DMSO/50% DMF.

Table 3: Porosity and Peak Pore Diameter as determined from mercury porosimetry for PCU scaffolds prepared by SCPL using fructose and gelatin as a porogen.

Porogen Type	Porosity (%)	Peak Pore Diameter (µm)
D-Fructose (30% DMSO)	83.7	162.0
D-Fructose (50% DMSO)	75.8	112.9
Gelatin	90.6	100.2

The mercury intrusion curves (Figure 12) supported the premise that an increase in DMSO concentration would result in increased microporosity within the resulting scaffold. At 30% DMSO concentration, the smallest pore sizes were approximately 10 μm in magnitude, while at a DMSO concentration of 50%, pore sizes as small as about 0.01 μm were observed. As was seen with SEM, micropores within the range of 30-10 μm existed at any solvent mixture concentration, including scaffolds fabricated with 100% DMF. However, these pores were scarce and could be derived form the nucleation and growth of solvent bubbles before evaporation, and/or phase separation caused by the presence of residual solvent during the particulate leaching step.[57] Through an increase in DMSO concentration, additional micropores were created as fructose molecules at the surface of the porogen particles began to migrate through the polymer/solvent solution during the solvent evaporation step of the scaffold fabrication process. This enhanced microporosity should increase mass transfer and intercellular communication within the construct, which could significantly improve the formation of 3D tissues and the *in vivo* performance of the tissue-engineered construct.[102]

In summary, it was shown that D-fructose particles could be used to fabricate scaffolds with a regular geometry of pores and enhanced microporosity by using a polymer solvent mixture of DMF and DMSO. The pore size and degree of microporosity could be tailored by altering the concentration of DMSO in the solvent mixture. The high microporosity and surface-area-to-volume ratio of scaffolds fabricated with a high DMSO concentration is advantageous since it could potentially

improve cell-attachment and mass transfer within the tissue-engineered construct. However, at DMSO concentrations as high as 50%, the regular distribution of pores was compromised and a non-uniform porosity was found within the scaffold. In addition, if microporosity is too high, it could potentially affect the mechanical properties of the scaffold. Thus, a balance must exist in order to maximize the desirable attributes without compromising scaffold uniformity and mechanical properties. One of the main advantages of this technique is that it is a simple way to induce an open-celled, spherical and regular pore geometry within the scaffold without any additional steps required in the fabrication process, such as heat treatment or spheronization of the sugar particles prior to SCPL.[66, 68]

4.3.3 Scaffolds Fabricated using Gelatin Spheres

Gelatin is a denatured product of collagen and contains bioactive sequences that can enhance positive cell–material interaction.[60] As such, it is a promising choice of porogen for scaffold fabrication, since residual gelatin remaining after porogen leaching could potentially be beneficial to cell growth. Several groups have reported the use of gelatin particles[60, 62, 63] and spheres[43, 61, 64, 71, 103] as porogens with promising results. In this work, scaffolds were fabricated using gelatin microspheres in order to evaluate their suitability for vascular tissue engineering applications and to directly compare their morphological characteristics with the previously discussed scaffolds fabricated from the same PCU.

Although it is dependent on the type of polymer used in scaffold fabrication, a problem often observed when using gelatin as a porogen is the lack of interconnectivity between pores.[61] Some researchers have improved interconnectivity by bonding the gelatin spheres (or particles) together through pretreatment methods.[43, 61, 62] Another group combined particulate leaching of gelatin spheres with a phase inversion (PI) technique.[103] Here, the effectiveness of the combined technique in improving interconnectivity was evaluated by fabricating scaffolds by the SCPL method as well as by the combined SCPL and PI technique. Figure 13A shows an SEM image of the purchased gelatin microspheres (120-150 μm), and Figure 13B shows the morphology of scaffolds fabricated using these microspheres and the SCPL technique. It can be seen that the vast majority of the pores are isolated from one another, which would drastically limit cell ingrowth. In contrast, Figures 13C and D show that scaffolds fabricated with the combined SCPL/PI technique have superior pore interconnectivity. In this method, instead of allowing the solvent to evaporate following solvent casting, the scaffold was immediately immersed in ethanol, a nonsolvent for both the polymer and the porogen. This results in a ternary polymer/solvent/nonsolvent phase separation in which the solvent (DMF) is exchanged for nonsolvent (ethanol), causing precipitation of the polymer. This process helps to improve the interconnection of pores in the resulting scaffold because the polymer chains retract from the gelatin spheres, preventing them from forming a thin layer between porogen contact points.

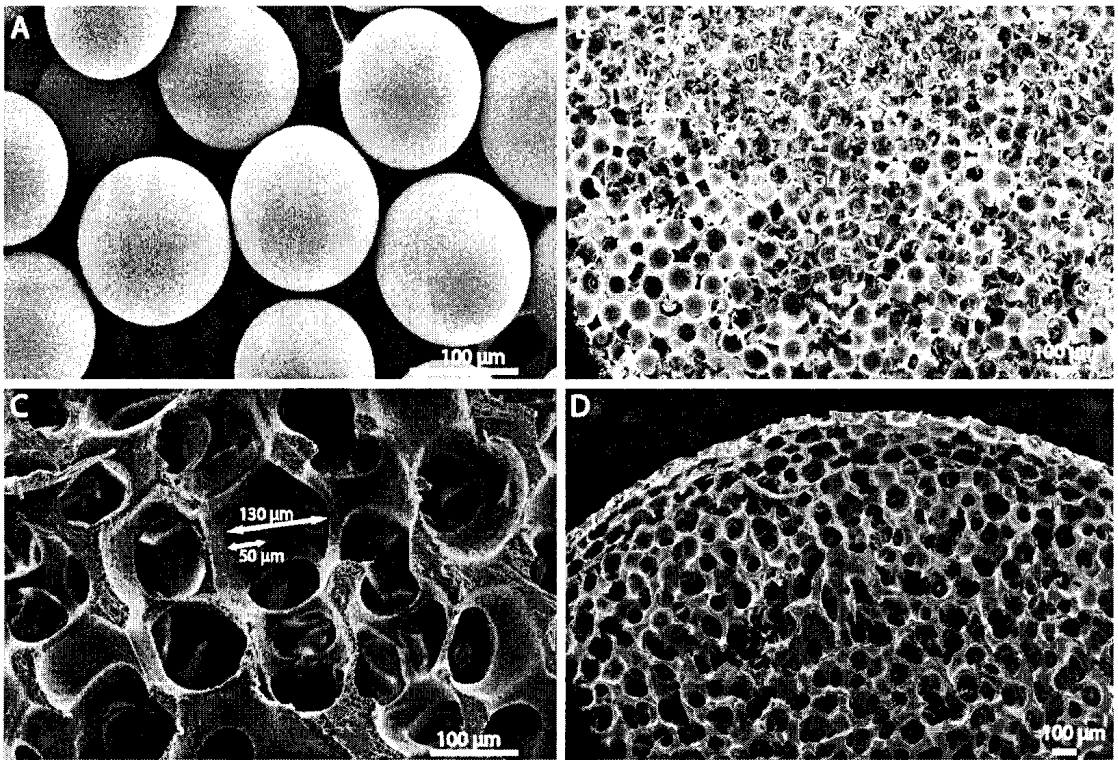

Figure 13: Purchased gelatin microspheres (120-150 µm) (A), and scaffold fabricated with gelatin microspheres using SCPL method (B) and SCPL/PI method (C-D). Example pore size and window size is indicated (C).

The phase inversion technique also typically creates micropores within the range of approximately 1 to 10 µm, and the extent of microporosity depends on the relative rates at which solvent is exchanged for nonsolvent.[103] Mercury porosimetry analysis was carried out on a scaffold fabricated using the combined SCPL/PI technique, and both SEM and mercury porosimetry analysis showed minimal presence of micropores (Figure 13C and Figure 14). This suggests that the nonsolvent (ethanol) enters the solution at a rate lower than that at which the solvent (DMF) leaves.[103] The degree of microporosity could potentially be tailored through the choice of nonsolvent.

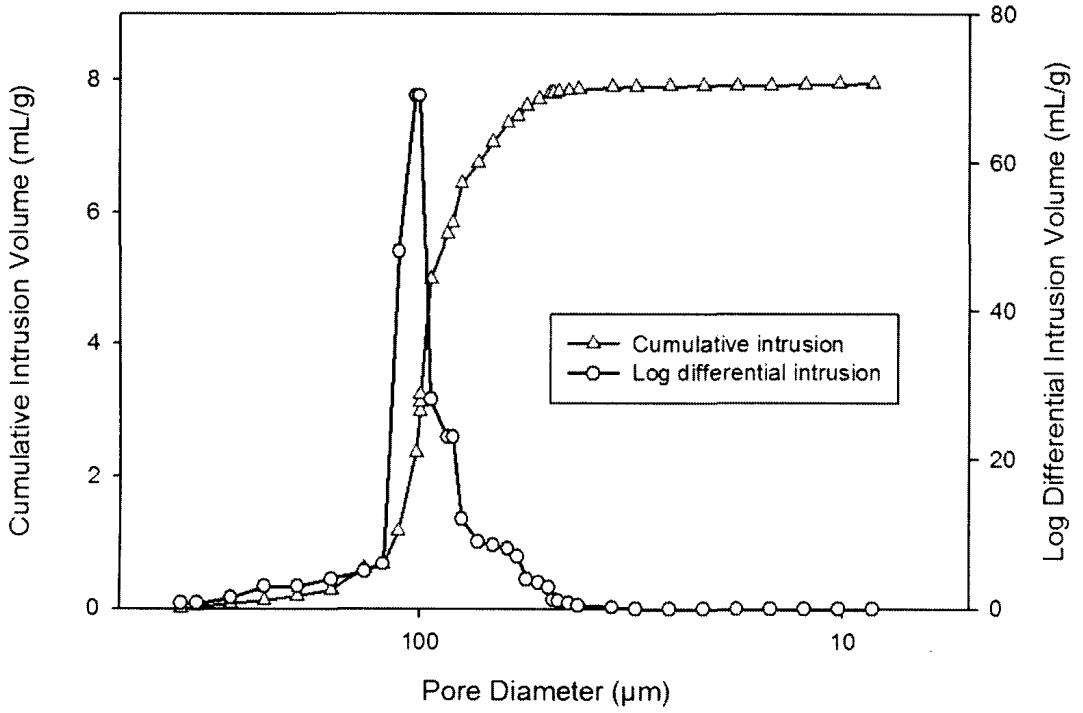

Figure 14: Mercury porosimetry results of scaffold fabricated using gelatin spheres and a combined SCPL/PI technique.

Through mercury porosimetry analysis, the peak pore diameter was determined to be 100.2 μm (Table 3), which is smaller than the lower limit gelatin sphere diameter of 120 μm. This can be understood by examining the pore architecture. Figure 13C shows that the interconnecting windows between pores are often smaller than the pore size itself (the example shows a window size of ~50 μm, and a pore size of ~130 μm). Thus, since the Washburn equation calculates pore diameters assuming a cylindrical pore, it underestimates the pore sizes for this kind of pore geometry.

From mercury porosimetry data, scaffold porosity was determined to be 90.6% (Table 3). This is a promising result because difficulties in obtaining high porosities while

using gelatin as a porogen have been reported.[64, 71] The high porosity obtained here could be attributed to the combination of tight packing of the gelatin spheres (imparted by the application of a pressure differential) and shrinkage of the PCU during the phase separation step.

4.4 Scaffolds Fabricated by Electrospinning

While scaffolds prepared by the solvent casting/particulate leaching method contain pores that are of a macro-sized scale as viewed by the cells, electrospinning offers the ability to fabricate scaffolds that closely mimic the scale and fibrous nature of the native extracellular matrix (ECM). Native ECM consists of nanoscaled protein fibers, such as collagen and elastin, which entangle with each other to form a nonwoven mesh that provides tensile strength and elasticity for the tissues.[40] Adhesive proteins that provide specific binding sites for cell adhesion, such as fibronectin and laminin, also exist as nanoscaled fibers in ECM.[40] Considerable research has indicated that these nanoscaled features influence cell behavior.[40, 81] From the electrospinning scaffold fabrication technique, fibers at the sub-micron and nanometer scale can be prepared, and since the diameters of these fibers are orders of magnitude smaller than the size of cells, cells are able to organize around the fibers or spread and attach to adsorbed proteins at multiple focal points.[81] These fiber matrices also have high surface-area-to-volume ratios, which allow for a high percentage of cellular attachment,[40, 81] and for many cell types cell migration, proliferation, and differentiated function are dependent on cell adhesion.[41, 98]

In view of these benefits, electrospun fiber mats were prepared in this study using the same PCU used to prepare the aforementioned SCPL scaffolds in order to evaluate and compare the effectiveness of these fabrication techniques. The polymer was spun at various conditions to determine the effects on the properties of the fibers, such as fiber diameter, which can affect cell attachment, proliferation, migration and cytoskeletal organization.[104]

Since polymer solution concentration has been reported to be one of the biggest determiners of fiber size and morphology when electrospinning,[81] the effects of solution concentration were studied here. Figure 15 shows SEM images of electrospun fibers prepared using a PCU concentration of 15 % (v/v), while Figure 16 shows the effect of altering the polymer solution concentration (PCU in DMF) on fiber diameter. Note that fiber morphology was the same at 10, 12.5, and 15% PCU concentration, so SEM analysis is shown for one of these concentrations only. It can be seen that there was a significant increase in mean fiber diameter when concentration was increased from 10 to 12.5%, while no significant difference was observed when concentration increased from 12.5 to 15% (Figure 16D). Electrospinning at concentrations above 15% was not possible, since the droplet at the tip of the needle dried out before jets could be stabilized. In addition, fibers could not be produced at or below a concentration of 5% because the fibers were still wet when they reached the collector.

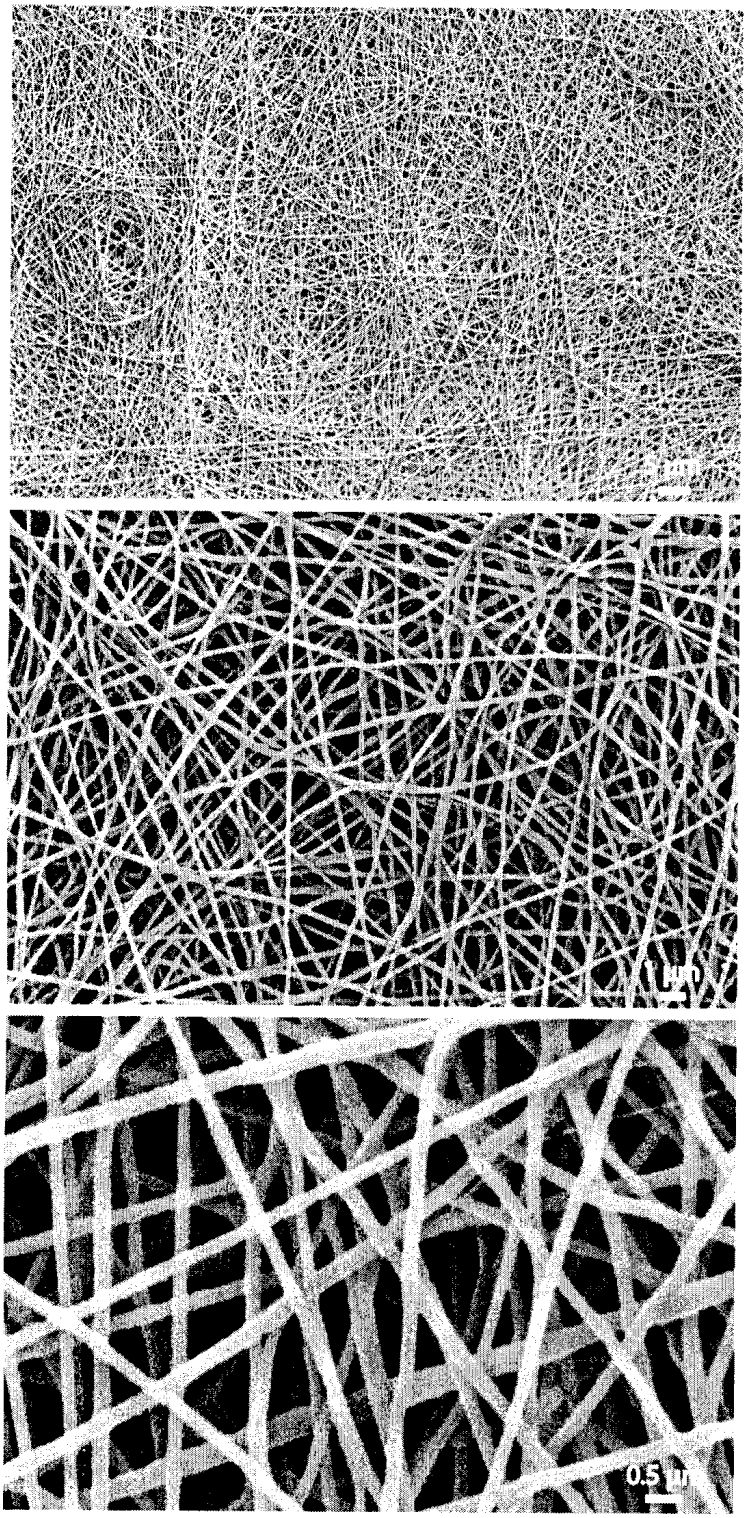

Figure 15: Different magnifications of PCU fibers prepared by electrospinning at the following conditions: 15% PCU, 15 kV voltage, 8 cm distance from collector, and 0.1 mL/h flowrate.

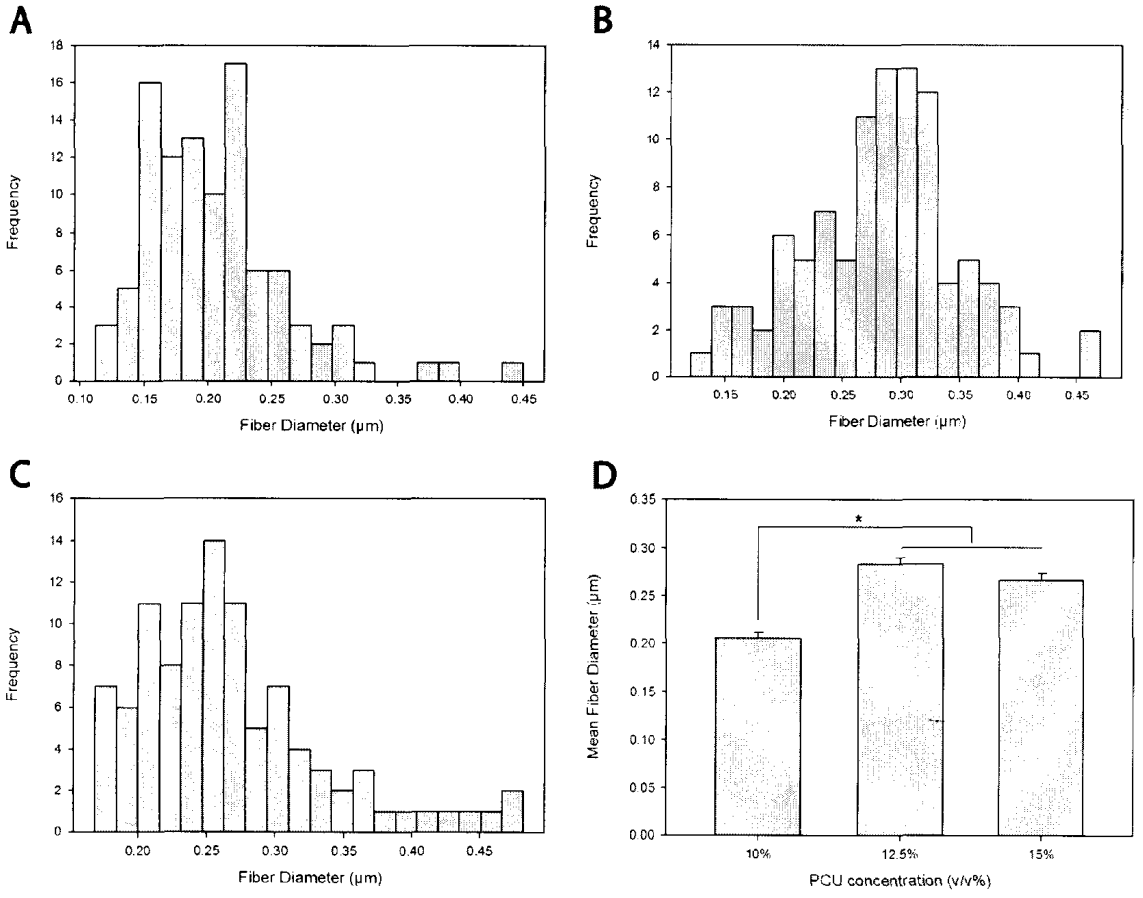

Figure 16: Fiber diameter distribution (N=100) of electrospun fibers prepared using 15 kV voltage, 8 cm distance from collector, 0.1 ml/h flowrate, and 10% PCU (A), 12.5% PCU (B), 15% PCU (C), and the effect of PCU concentration on mean fiber diameter (D). Data expressed as mean ± standard error. Statistical significance ($p<0.05$) indicated by *.

The resulting morphology of PCU spun at a concentration of 5% is shown in Figure 17. These clusters of beads and droplets formed at low polymer concentrations are characteristic of electrospraying, whereby the jet breaks into droplets.[81, 82]

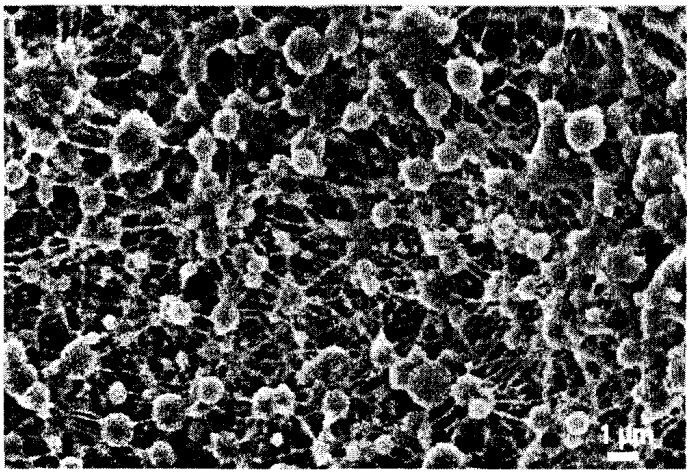

Figure 17: SEM image of electrospun PCU at the following conditions: 5% PCU, 15 kV voltage, 8 cm distance, and 0.1 ml/h flowrate.

Between these concentration limits, however, promising results were obtained. At 10, 12.5, and 15% PCU concentration, mean fiber diameters of 205, 283, and 267 nm respectively were obtained. This is desirable because when electrospinning tissue engineering scaffolds, nanofibers with diameters from several tens to 300 nm, the typical diameter of protein fibril/fibers in native ECM, are usually preferred.[40] Furthermore, another important feature is that the fibers obtained were very uniform in diameter (see Figure 16). This is a key point because precise control of fiber morphology and fiber diameter uniformity have proven difficult to achieve, yet are necessary for improved scaffold designs that better recreate the functions of native extracellular matrix.[81] For example, one group reported that when electrospinning 12.8 wt% polyurethaneurea solutions, an approximate trimodal distribution in fiber diameter was observed, whereby fibers ranged from less than 0.5 μm to greater than 1.4 μm in diameter.[82] In contrast, in this study, narrower fiber diameter distributions,

which were more normally distributed, were obtained, as can be seen in Figures 16A-C.

The effect of voltage on fiber diameter and morphology was also examined in this study. Figures 18A-C show SEM images of electrospun PCU at three different voltages (note that all other conditions remained constant).

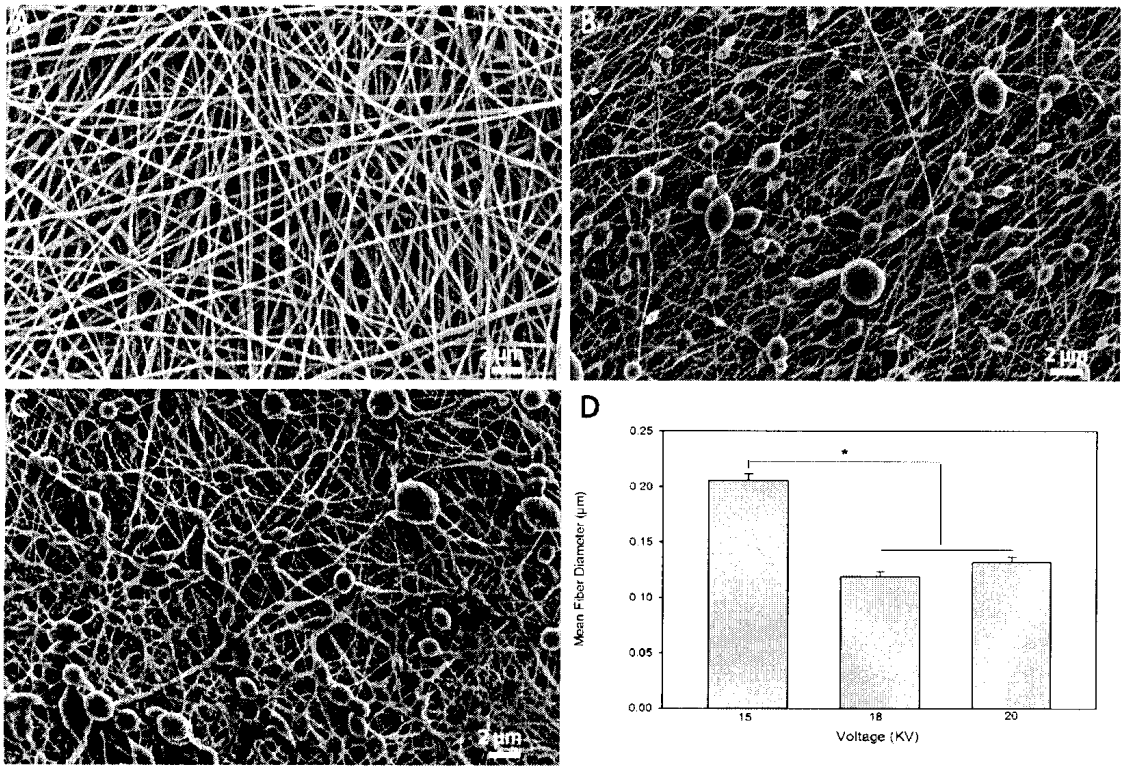

Figure 18: Electrospun PCU at 10% PCU, 8cm distance from collector, 0.1 ml/h flowrate, and a voltage of 15 kV (A), 18 kV (B), 20 kV (C), and effect of voltage on mean fiber diameter (D). Data expressed as mean ± standard error. * indicates statistical significance ($p<0.05$).

It can be seen that an increase in voltage caused bead formation; however, in order to get an idea of the effect of voltage on fiber diameter, fiber diameter measurements were made excluding the beads, and the results indicated that fiber diameter decreases with voltage (Figure 16D). Bead formation has been said to stem mainly from the high electrical field applied to the system.[82] For tissue engineering scaffolds, beads are not desirable because they significantly reduce scaffold uniformity and decrease the surface area to volume ratio.[82] Beads were also formed when the flowrate was increased from 0.1 mL/h to 0.15 mL/h (see Figure 19). The increased flowrate did not allow enough time for solvent evaporation, which resulted in bead formation. Flowrates below 0.1 mL/h were not considered practical due to the time required to prepare fiber mats.

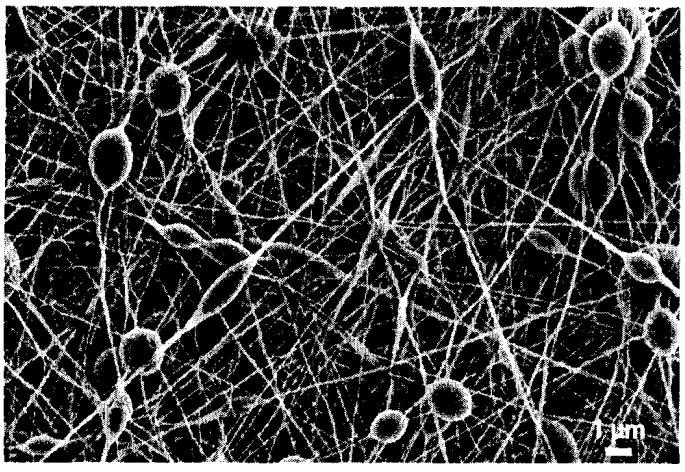

Figure 19: SEM image of electrospun PCU at the following conditions: 10% PCU, 15 kV voltage, 8cm distance, and 0.15 mL/h flowrate.

4.5 Vascular Smooth Muscle Cell Culture Studies

Cytotoxicity and cell spreading were the two main focuses for conducting preliminary cell culture studies. First, when using the SCPL scaffold fabrication method, residual amounts of the porogen material could remain within the scaffold following processing. This can happen due to the possibility of porogen entrapment in the polymer matrix or due to insufficient leaching.[60] Therefore, it is important to ensure that any residual porogen or solvent left following scaffold fabrication are not toxic to cells. The second focus was to observe the effect of scaffold properties, namely morphological characteristics, on cellular attachment and spreading.

Human coronary artery smooth muscle cells (HCASMCs) were used to carry out preliminary cell studies on 3D PCU scaffolds. The rationale for using HCASMCs is based on our long-term objective of fabricating a human vascular tissue model with clinical relevance. The scaffolds chosen were those fabricated by: (1) SCPL using alginate beads; (2) SCPL using D-fructose (30% DMSO); and (3) electrospinning (15% PCU, 15 kV voltage, 8 cm distance from collector, and 0.1 mL/h flowrate). The morphology of these scaffolds was presented in Figures 6, 9D, and 15, respectively. For the scaffold fabricated using D-fructose, a solvent mixture concentration of 30% DMSO/70% DMF was used because the DMSO concentration was such that the resulting scaffolds had spherically shaped pores without compromising the overall scaffold integrity.

For cytotoxicity tests, MTT assay was used to determine cell number. This method is based on the reduction of yellow tetrazolium salt (MTT) to purple formazan crystal by metabolically active cells.[105] The reduction occurs when mitochondrial reductase enzymes are active, meaning conversion can be directly related to the number of viable cells. After the formazan is solubilised, resulting in a colored solution, its concentration can be determined though optical density measurements at 570 nm. The resulting colorimetric signal is proportional to the cell number. Cytotoxicity data were obtained following 7 and 14 days of culture. The results are shown in two different ways in order to compare the effect of both scaffold fabrication method (Figure 20) and culture time (Figure 21).

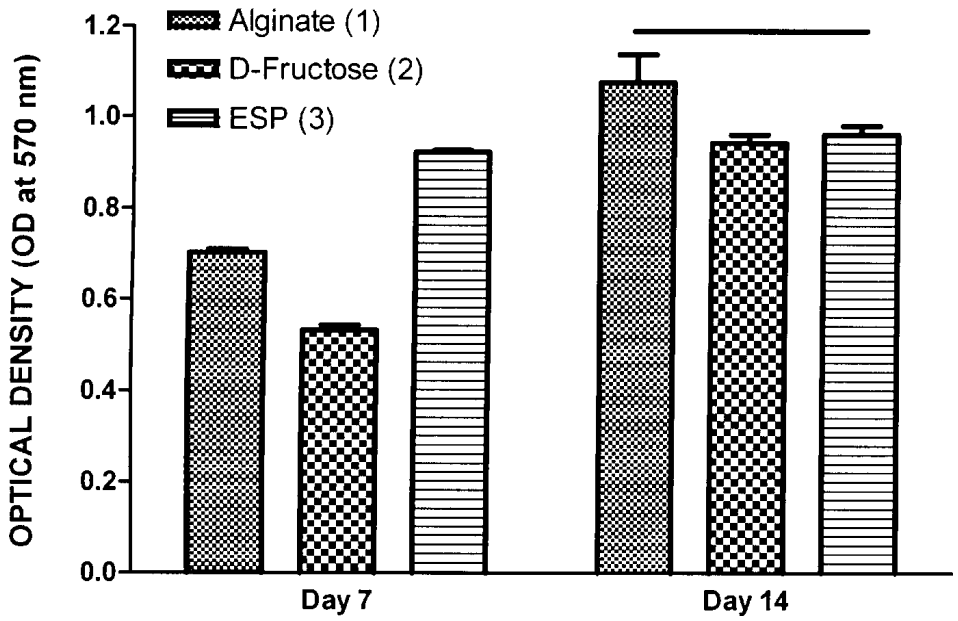

Figure 20: Effect of scaffold fabrication method on HCASMC viability on 3D PCU scaffolds fabricated by (1) SCPL using alginate beads, (2) SCPL using D-Fructose (30% DMSO), and (3) by electrospinning (15% PCU, 15 kV voltage, 8 cm distance from collector, and 0.1 mL/h flowrate). Data expressed as mean ± SD for experiments conducted in quadruplicate. One way ANOVA and post-hoc Tukey comparative tests were used. Solid line indicates data that are not statistically significant.

At day 7 there was a statistically significant difference in cell viability between all three scaffold fabrication methods, with electropun (ESP) scaffolds having the highest cell viability and scaffolds prepared using D-fructose having the lowest (Figure 20). In contrast, at day 14, there was no statistical significance in cell viability between any of the three different fabrication methods. The much higher cell viability at day 7 for electrospun scaffolds when compared to those prepared by SCPL was likely due to the higher surface area available for cell attachment. Previous studies have indicated that scaffolds fabricated by electrospinning have higher surface-area-to-volume ratios than those fabricated by SCPL.[98] The statistical significance in cell number between scaffolds fabricated using alginate beads and those fabricated using D-fructose may also be explained by their statistical significance in surface-area-to-volume ratio. Scaffolds prepared using alginate beads were found to have a surface-area-to-volume ratio of 84.7 ± 20.5 mm^{-1}, while scaffolds prepared using D-fructose (30% DMSO) had a significantly lower surface-area-to-volume ratio of 68.3 ± 11.3 mm^{-1} (refer to Table 2). Another possible reason for the higher cell viability at day 7 for scaffolds fabricated using alginate beads than those fabricated using D-fructose is the presence of residual porogen material. Yu and Fan reported that, following fabrication of PLA scaffolds by SCPL using alginate beads as a porogen, the existence of alginate molecules on the surface of scaffolds significantly enhanced osteoblast adhesion and proliferation.[69] Thus, residual alginate on the surface of scaffolds likely enhances cell attachment for scaffolds prepared using alginate beads.

Although cell viability was initially much higher for electrospun scaffolds, there was no statistical difference in cell viability between any of the three scaffolds at day 14. Cell number for scaffolds fabricated by SCPL increased significantly between 7 and 14 days of culture but remained constant for electrospun scaffolds (Figure 21). This is an interesting observation that suggests that the large differences in scaffold morphology between electrospun scaffolds and those fabricated by SCPL affect cellular responses.

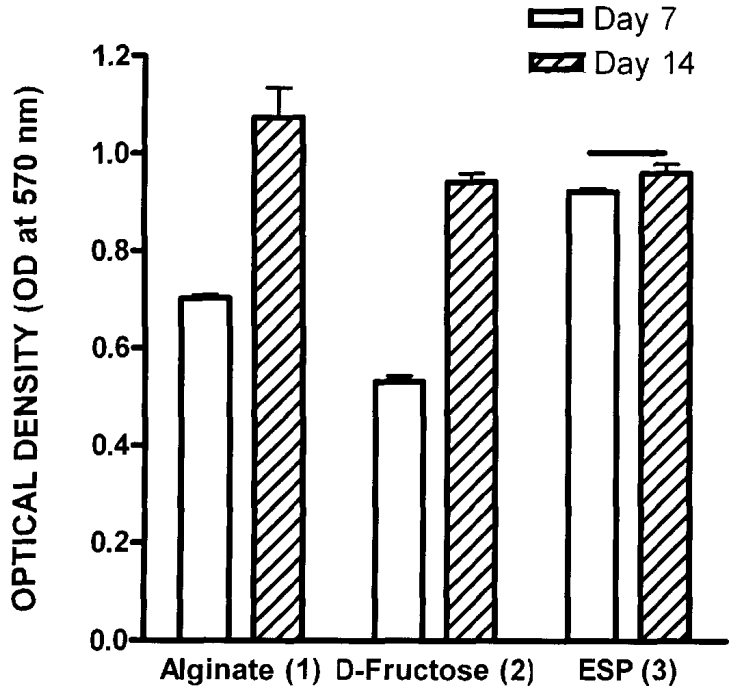

Figure 21: Effect of culture time on HCASMC viability on 3D PCU scaffolds fabricated by (1) SCPL using alginate beads, (2) SCPL using D-Fructose (30% DMSO), and (3) by electrospinning (15% PCU, 15 kV voltage, 8 cm distance from collector, and 0.1 mL/h flowrate). Data expressed as mean ± SD for experiments conducted in quadruplicate. One way ANOVA and post-hoc Tukey comparative tests were used. Solid line indicates data that are not statistically significant.

The lower proliferation rate observed on the electrospun scaffolds is likely caused by differences in gene and/or phenotype expression imparted by differences in

morphological characteristics. The major difference between electrospun scaffolds and those fabricated by SCPL is that the former contains pores that are smaller than the size of cells, while the in the case of the latter the majority of the pores are larger than the size of cells. This difference is a factor because it is believed that if pore sizes are similar or larger than that of cells (~5-30 μm diameter), cells behave as if in a 2D environment with a curvature, and that in order for cells to behave as in a true 3D environment, the scaffold's fibers and/or pores must be much smaller than the cells.[106] In view of this, it is reasonable to assume that differences in cell behavior observed on the electrospun scaffolds when compared with the scaffolds fabricated by SCPL may be comparable to differences that have been previously observed when comparing 2D and 3D scaffold environments. One such report indicated that human aortic smooth muscle cells cultured on 3D collagen matrices had a lower proliferation rate than when cultured on 2D surfaces.[107] Their studies indicated that this was due to the lower expression levels of genes involved in cell cycle in the 3D matrix. Taken altogether, preliminary cell studies showed that between 7 and 14 days of culture, cells were less proliferative on electrospun scaffolds than those prepared by SCPL, and this could support the notion that scaffolds with pores and/or fibers smaller than that of the cells provide an environment more like that of true 3D.

Cell morphology was examined after 7 days of culture using confocal microscopy, and the results are shown in Figure 22. For all three scaffolds, cells appeared well-spread with abundant F-actin.

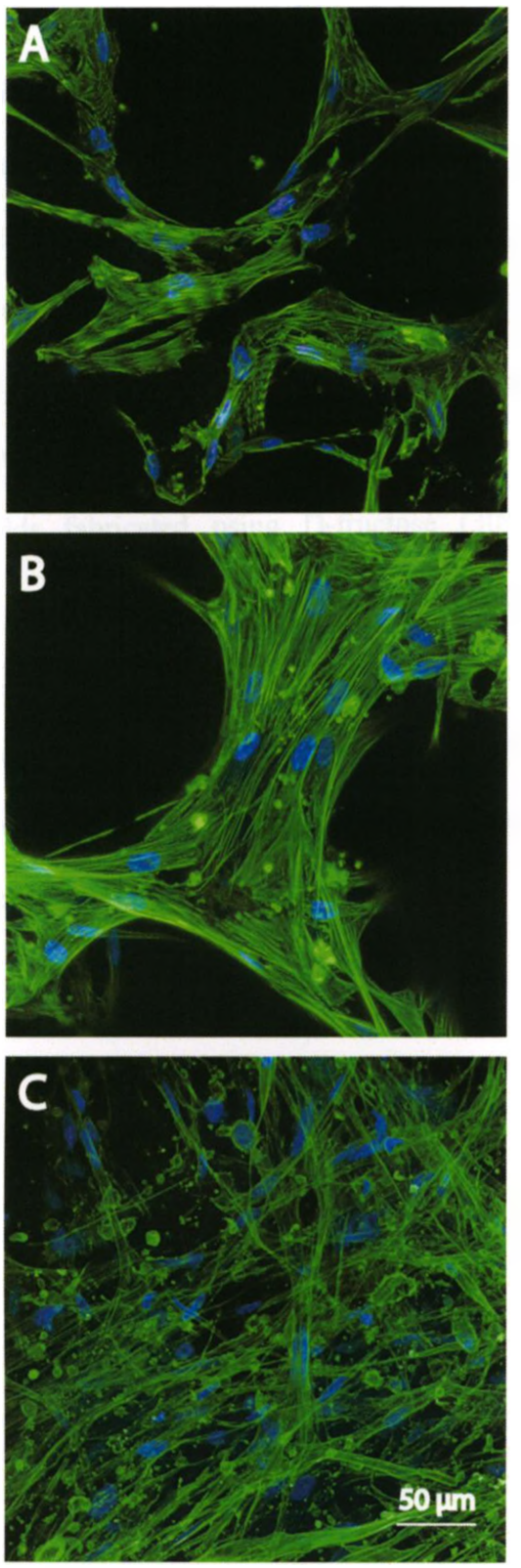

Figure 22: Representative confocal microscopy images of HCASMCs cultured for 7 days on 3D PCU scaffolds fabricated by SCPL using alginate beads (A), SCPL using D-fructose (30% DMSO) (B), and by electrospinning (15% PCU, 15 kV voltage, 8 cm distance from collector, and 0.1 mL/h flowrate) (C). Green represents F-actin (phalloidin stained) and blue is for nuclei.

For the scaffolds fabricated by SCPL (Figures 22A & B), it can be seen that cells align along the struts, while for the electrospun scaffold, cells spread along the fibers and thus have a larger area for cell attachment and spreading (Figure 22C). When comparing the scaffolds fabricated by SCPL using the two porogen types, it appears that scaffolds fabricated using D-fructose (Figure 22B) are more densely populated with cells than scaffolds fabricated using alginate beads (Figure 22A). This is contrary to what was found with MTT assay and may be a result of the difference in pore size, since scaffolds fabricated using D-fructose (30% DMSO) have a significantly larger pore size (172.1 ± 36.3 μm) than the scaffolds fabricated using alginate beads (146.7 ± 34.3 μm) (Table 2), and as such, cells appear more densely populated along the struts even if overall cell number is not high. Despite this difference, preliminary cell studies indicated a favorable environment for cell growth on all three different types of scaffolds examined.

CHAPTER 5

5 Conclusions and Future Directions

5.1 Conclusions

In this study, 3D scaffolds were fabricated from biostable polyurethane by solvent casting/particulate leaching and by electrospinning. Scaffolds fabricated using SCPL were fabricated using three different types of porogens: alginate beads, D-fructose particles, and gelatin spheres. The alginate beads were successfully prepared within the desired size range by an emulsification and ionic gelation technique. Using alginate beads as a porogen, highly porous scaffolds with well-interconnected and spherical pores were fabricated without the need for any additional processing steps. By using D-fructose as a porogen, a novel method of tailoring scaffold morphological characteristics such as scaffold microporosity, and pore size and shape was established. Scaffolds prepared using gelatin spheres as a porogen had a closed pore morphology; however, when using a combined SCPL/phase inversion technique, the resulting scaffolds had open-celled pore morphology. 3D scaffolds were also fabricated by elecrospinning, whereby the fibrous mats had a narrow fiber diameter distribution and mean fiber diameters of approximately 200 nm. HCASMC culture studies carried out on scaffolds fabricated by electrospinning and by SCPL using alginate and D-fructose as a porogen indicated that the scaffolds were not cytotoxic and that the large difference in morphological characteristics between scaffolds

fabricated by SCPL and those fabricated by electrospinning can significantly affect cell behavior.

Developing scaffolds to suit the intended application is crucial to the success of tissue engineering. In this study, the morphological properties of scaffolds fabricated by a variety of methods were examined, and the findings could not only be valuable in contributing to the long-term goal of developing fully functional tissue engineered vascular constructs for clinical use but may also be extended to other scaffold-dependent applications within the field of tissue engineering.

5.2 Future Directions

The different scaffolds fabricated in this study were evaluated in terms of their morphology, but their mechanical properties were not evaluated. In the future, it would be beneficial to study the effect of different morphological characteristics, such as microporosity, on the mechanical properties of the scaffold. In addition, further cell studies should be carried out in order to examine the effects of scaffold morphology and residual porogen material on cell behavior, such as protein and cell phenotype expression.

References

1. Sachlos, E.; Czernuszka, J. T., Making tissue engineering scaffolds work. Review: the application of solid freeform fabrication technology to the production of tissue engineering scaffolds. *Eur Cell Mater* **2003,** 5, 29-39; discussion 39-40.
2. Courtney, T.; Sacks, M. S.; Stankus, J.; Guan, J.; Wagner, W. R., Design and analysis of tissue engineering scaffolds that mimic soft tissue mechanical anisotropy. *Biomaterials* **2006,** 27, (19), 3631-8.
3. Langer, R.; Vacanti, J. P., Tissue engineering. *Science* **1993,** 260, (5110), 920-6.
4. Rabkin, E.; Schoen, F. J., Cardiovascular tissue engineering. *Cardiovasc Pathol* **2002,** 11, (6), 305-17.
5. L'Heureux, N.; Pâquet, S.; Labbé, R.; Germain, L.; Auger, F. A., A completely biological tissue-engineered human blood vessel. *FASEB J* **1998,** 12, (1), 47-56.
6. El Oakley, R. M.; Ooi, O. C.; Bongso, A.; Yacoub, M. H., Myocyte transplantation for myocardial repair: a few good cells can mend a broken heart. *Ann Thorac Surg* **2001,** 71, (5), 1724-33.
7. Pankajakshan, D.; Agrawal, D. K., Scaffolds in tissue engineering of blood vessels. *Can J Physiol Pharmacol* **2010,** 88, (9), 855-73.
8. Meinhart, J. G.; Deutsch, M.; Fischlein, T.; Howanietz, N.; Fröschl, A.; Zilla, P., Clinical autologous in vitro endothelialization of 153 infrainguinal ePTFE grafts. *Ann Thorac Surg* **2001,** 71, (5 Suppl), S327-31.
9. Miller, W. M.; Peshwa, M. V., Tissue engineering, bioartificial organs, and cell therapies: *Biotechnol Bioeng* **1996,** 50, (4), 347-8.
10. L'Heureux, N.; McAllister, T. N.; de la Fuente, L. M., Tissue-engineered blood vessel for adult arterial revascularization. *N Engl J Med* **2007,** 357, (14), 1451-3.

11. Atala, A.; Bauer, S. B.; Soker, S.; Yoo, J. J.; Retik, A. B., Tissue-engineered autologous bladders for patients needing cystoplasty. *Lancet* **2006,** 367, (9518), 1241-6.

12. Macchiarini, P.; Jungebluth, P.; Go, T.; Asnaghi, M. A.; Rees, L. E.; Cogan, T. A.; Dodson, A.; Martorell, J.; Bellini, S.; Parnigotto, P. P.; Dickinson, S. C.; Hollander, A. P.; Mantero, S.; Conconi, M. T.; Birchall, M. A., Clinical transplantation of a tissue-engineered airway. *Lancet* **2008,** 372, (9655), 2023-30.

13. Kusuma, S.; Gerecht, S., Engineering blood vessels using stem cells: innovative approaches to treat vascular disorders. *Expert Rev Cardiovasc Ther* **2010,** 8, (10), 1433-45.

14. Hoenig, M. R.; Campbell, G. R.; Rolfe, B. E.; Campbell, J. H., Tissue-engineered blood vessels: alternative to autologous grafts? *Arterioscler Thromb Vasc Biol* **2005,** 25, (6), 1128-34.

15. Roger, V. L.; Go, A. S.; Lloyd-Jones, D. M.; Adams, R. J.; Berry, J. D.; et al., Heart Disease and Stroke Statistics--2011 Update: A Report From the American Heart Association. *Circulation* **2011,** 123, (4), e18-e209.

16. Grenier, S.; Sandig, M.; Holdsworth, D. W.; Mequanint, K., Interactions of coronary artery smooth muscle cells with 3D porous polyurethane scaffolds. *J Biomed Mater Res Part A* **2009,** 89, (2), 293-303.

17. Beamish, J. A.; He, P.; Kottke-Marchant, K.; Marchant, R. E., Molecular regulation of contractile smooth muscle cell phenotype: implications for vascular tissue engineering. *Tissue Engineering Part B: Reviews* **2010,** 16, (5), 467-91.

18. Grenier, S.; Sandig, M.; Mequanint, K., Polyurethane biomaterials for fabricating 3D porous scaffolds and supporting vascular cells. *J Biomed Mater Res Part A* **2007,** 82, (4), 802-9.

19. Vara, D. S.; Salacinski, H. J.; Kannan, R. Y.; Bordenave, L.; Hamilton, G.; Seifalian, A. M., Cardiovascular tissue engineering: state of the art. *Pathol Biol* **2005,** 53, (10), 599-612.

20. Petersen, M. C.; Lazar, J.; Jacob, H. J.; Wakatsuki, T., Tissue engineering: a new frontier in physiological genomics. *Physiological Genomics* **2007,** 32, (1), 28-32.

21. Kim, J. B., Three-dimensional tissue culture models in cancer biology. *Semin Cancer Biol* **2005,** 15, (5), 365-77.

22. Schanz, J.; Pusch, J.; Hansmann, J.; Walles, H., Vascularised human tissue models: a new approach for the refinement of biomedical research. *J Biotechnol* **2010,** 148, (1), 56-63.

23. Hansen, A.; Eder, A.; Bönstrup, M.; Flato, M.; Mewe, M.; Schaaf, S.; Aksehirlioglu, B.; Schwörer, A.; Uebeler, J.; Eschenhagen, T., Development of a drug screening platform based on engineered heart tissue. *Circ Res* **2010,** 107, (1), 35-44.

24. L'Heureux, N.; Stoclet, J. C.; Auger, F. A.; Lagaud, G. J.; Germain, L.; Andriantsitohaina, R., A human tissue-engineered vascular media: a new model for pharmacological studies of contractile responses. *FASEB J* **2001,** 15, (2), 515-24.

25. Katare, R. G.; Ando, M.; Kakinuma, Y.; Sato, T., Engineered heart tissue: a novel tool to study the ischemic changes of the heart in vitro. *PLoS ONE* **2010,** 5, (2), e9275.

26. Huh, D.; Matthews, B. D.; Mammoto, A.; Montoya-Zavala, M.; Hsin, H. Y.; Ingber, D. E., Reconstituting organ-level lung functions on a chip. *Science* **2010,** 328, (5986), 1662-8.

27. Reichl, S.; Döhring, S.; Bednarz, J.; Müller-Goymann, C. C., Human cornea construct HCC-an alternative for in vitro permeation studies? A comparison with human donor corneas. *Eur J Pharm Biopharm* **2005,** 60, (2), 305-8.

28. Verbridge, S. S.; Choi, N. W.; Zheng, Y.; Brooks, D. J.; Stroock, A. D.; Fischbach, C., Oxygen-controlled three-dimensional cultures to analyze tumor angiogenesis. *Tissue Eng Part A* **2010,** 16, (7), 2133-41.

29. Raimondi, M. T., Engineered tissue as a model to study cell and tissue function from a biophysical perspective. *Curr Drug Discov Technol* **2006,** 3, (4), 245-68.

30. Yang, S.; Leong, K. F.; Du, Z.; Chua, C. K., The design of scaffolds for use in tissue engineering. Part I. Traditional factors. *Tissue Eng* **2001,** 7, (6), 679-89.

31. Carletti, E.; Motta, A.; Migliaresi, C., Scaffolds for tissue engineering and 3D cell culture. *Methods Mol Biol* **2011,** 695, 17-39.

32. Tran, S. C.; Cooley, A. J.; Elder, S. H., Effect of a mechanical stimulation bioreactor on tissue engineered, scaffold-free cartilage. *Biotechnol. Bioeng.* **2011,** 108, (6), 1421-9.

33. Norotte, C.; Marga, F. S.; Niklason, L. E.; Forgacs, G., Scaffold-free vascular tissue engineering using bioprinting. *Biomaterials* **2009,** 30, (30), 5910-7.

34. Kelm, J. M.; Lorber, V.; Snedeker, J. G.; Schmidt, D.; Broggini-Tenzer, A.; Weisstanner, M.; Odermatt, B.; Mol, A.; Zünd, G.; Hoerstrup, S. P., A novel concept for scaffold-free vessel tissue engineering: self-assembly of microtissue building blocks. *J Biotechnol* **2010,** 148, (1), 46-55.

35. Gurkan, U. A.; Kishore, V.; Condon, K. W.; Bellido, T. M.; Akkus, O., A scaffold-free multicellular three-dimensional in vitro model of osteogenesis. *Calcif Tissue Int* **2011,** 88, (5), 388-401.

36. Chaterji, S.; Park, K.; Panitch, A., Scaffold-free in vitro arterial mimetics: the importance of smooth muscle-endothelium contact. *Tissue Eng Part A* **2010,** 16, (6), 1901-12.

37. Owen, S. C.; Shoichet, M. S., Design of three-dimensional biomimetic scaffolds. *J Biomed Mater Res* **2010,** 94, (4), 1321-31.

38. Andersson, K.-E.; Christ, G. J., Regenerative pharmacology: the future is now. *Mol Interv* **2007,** 7, (2), 79-86.

39. Hutmacher, D. W., Scaffolds in tissue engineering bone and cartilage. *Biomaterials* **2000,** 21, (24), 2529-43.

40. Ma, Z.; Kotaki, M.; Inai, R.; Ramakrishna, S., Potential of nanofiber matrix as tissue-engineering scaffolds. *Tissue Eng* **2005,** 11, (1-2), 101-9.

41. Zhang, R.; Ma, P. X., Synthetic nano-fibrillar extracellular matrices with predesigned macroporous architectures. *J Biomed Mater Res* **2000,** 52, (2), 430-8.

42. Mooney, D. J.; Baldwin, D. F.; Suh, N. P.; Vacanti, J. P.; Langer, R., Novel approach to fabricate porous sponges of poly(D,L-lactic-co-glycolic acid) without the use of organic solvents. *Biomaterials* **1996,** 17, (14), 1417-22.

43. Draghi, L.; Resta, S.; Pirozzolo, M. G.; Tanzi, M. C., Microspheres leaching for scaffold porosity control. *J Mater Sci, Mater Med* **2005,** 16, (12), 1093-7.

44. Buckley, C. T.; O'Kelly, K. U., Regular scaffold fabricaton techniques for investigations in tissue engineering. *Topics in Bio-Mechanical Engineering* **2004**, 147-166.

45. Patel, A.; Fine, B.; Sandig, M.; Mequanint, K., Elastin biosynthesis: The missing link in tissue-engineered blood vessels. *Cardiovasc Res* **2006,** 71, (1), 40-9.

46. Vats, A.; Tolley, N. S.; Polak, J. M.; Gough, J. E., Scaffolds and biomaterials for tissue engineering: a review of clinical applications. *Clin Otolaryngol Allied Sci* **2003,** 28, (3), 165-72.

47. Mikos, A. G.; Temenoff, J., Formation of highly porous biodegradable scaffolds for tissue engineering. *Elect J Biotechnol* **2000**, 1-6.

48. Mikos, A.; Bao, Y.; Cima, L.; Ingber, D.; Vacanti, J.; Langer, R., Preparation of poly(glycolic acid) bonded fiber structures for cell attachment and transplantation. *J Biomed Mater Res* **1993,** 27, (2), 183-189.

49. Lu, L.; Mikos, A., The importance of new processing techniques in tissue engineering. *MRS Bull* **1996,** 21, (11), 28-32.

50. Mooney, D. J.; Mazzoni, C. L.; Breuer, C.; McNamara, K.; Hern, D.; Vacanti, J. P.; Langer, R., Stabilized polyglycolic acid fibre-based tubes for tissue engineering. *Biomaterials* **1996,** 17, (2), 115-24.

51. Schugens, C.; Maquet, V.; Grandfils, C.; Jerome, R.; Teyssie, P., Polylactide macroporous biodegradable implants for cell transplantation. II. Preparation of polylactide foams by liquid-liquid phase separation. *J Biomed Mater Res* **1996,** 30, (4), 449-461.

52. Reignier, J.; Huneault, M., Preparation of interconnected poly(3-caprolactone) porous scaffolds by a combination of polymer and salt particulate leaching. *Polymer* **2006,** 47.

53. Nam, Y. S.; Park, T. G., Biodegradable polymeric microcellular foams by modified thermally induced phase separation method. *Biomaterials* **1999,** 20, (19), 1783-90.

54. Liu, X.; Ma, P. X., Phase separation, pore structure, and properties of nanofibrous gelatin scaffolds. *Biomaterials* **2009,** 30, (25), 4094-103.

55. Whang, K.; Thomas, C.; Healy, K., A novel method to fabricate bioabsorbable scaffolds. *Polymer* **1995,** 36, (4), 837-42.

56. Mikos, A.; Thorsen, A.; Czerwonka, L.; Bao, Y.; Langer, R.; Winslow, D.; Vacanti, J., Preparation and characterization of poly(L-lactic acid) foams. *Polymer* **1994,** 35, (5), 1068-77.

57. Shastri, V. P.; Martin, I.; Langer, R., Macroporous polymer foams by hydrocarbon templating. *Proc Natl Acad Sci USA* **2000,** 97, (5), 1970-5.

58. Ma, P.; Choi, J., Biodegradable Polymer Scaffolds with Well-Defined Interconnected Spherical Pore Network. *Tissue Eng* **2001,** 7(1), 1-16.

59. Johnson, T.; Bahrampourian, R.; Patel, A.; Mequanint, K., Fabrication of highly porous tissue-engineering scaffolds using selective spherical porogens. *Biomed Mater Eng* **2010,** 20, (2), 107-18.

60. Gong, Y.; Ma, Z.; Zhou, Q.; Li, J.; Gao, C.; Shen, J., Poly(lactic acid) scaffold fabricated by gelatin particle leaching has good biocompatibility for chondrogenesis. *J Biomater Sci Polymer Edn* **2008,** 19, (2), 207-21.

61. Liu, X.; Won, Y.; Ma, P. X., Porogen-induced surface modification of nano-fibrous poly(L-lactic acid) scaffolds for tissue engineering. *Biomaterials* **2006,** 27, (21), 3980-7.

62. Zhou, Q.; Gong, Y.; Gao, C., Microstructure and mechanical properties of poly(L-lactide) scaffolds fabricated by gelatin particle leaching method. *J Appl Polym Sci* **2005,** 98, (3), 1373-1379.

63. Suh, S. W.; Shin, J. Y.; Kim, J.; Kim, J.; Beak, C. H.; Kim, D.-I.; Kim, H.; Jeon, S. S.; Choo, I.-W., Effect of different particles on cell proliferation in polymer scaffolds using a solvent-casting and particulate leaching technique. *ASAIO J* **2002,** 48, (5), 460-4.

64. Thomson, R. C.; Yaszemski, M. J.; Powers, J. M.; Mikos, A. G., Hydroxyapatite fiber reinforced poly(alpha-hydroxy ester) foams for bone regeneration. *Biomaterials* **1998,** 19, (21), 1935-43.

65. Misra, S. K.; Ansari, T. I.; Valappil, S. P.; Mohn, D.; Philip, S. E.; Stark, W. J.; Roy, I.; Knowles, J. C.; Salih, V.; Boccaccini, A. R., Poly(3-hydroxybutyrate) multifunctional composite scaffolds for tissue engineering applications. *Biomaterials* **2010,** 31, (10), 2806-15.

66. Capes, J. S.; Ando, H. Y.; Cameron, R. E., Fabrication of polymeric scaffolds with a controlled distribution of pores. *J Mater Sci, Mater Med* **2005,** 16, (12), 1069-75.

67. Wei, G.; Ma, P. X., Macroporous and nanofibrous polymer scaffolds and polymer/bone-like apatite composite scaffolds generated by sugar spheres. *J of Biomed Mater Res Part A* **2006,** 78, (2), 306-15.

68. Vaquette, C.; Frochot, C.; Rahouadj, R.; Wang, X., An innovative method to obtain porous PLLA scaffolds with highly spherical and interconnected pores. *J Biomed Mater Res Part B Appl Biomater* **2008,** 86, (1), 9-17.

69. Yu, G.; Fan, Y., Preparation of poly(D,L-lactic acid) scaffolds using alginate particles. *J Biomater Sci Polymer Edn* **2008,** 19, (1), 87-98.

70. Pankajakshan, D.; Philipose, L. P.; Palakkal, M.; Krishnan, K.; Krishnan, L. K., Development of a fibrin composite-coated poly(epsilon-caprolactone) scaffold for potential vascular tissue engineering applications. *J Biomed Mater Res Part B Appl Biomater* **2008,** 87, (2), 570-9.

71. Thomson, R.; Yaszemski, M.; Powers, J.; Mikos, A., Fabrication of biodegradable polymer scaffolds to engineer trabecular bone. *J Biomater Sci Polym Ed* **1995,** 7, (1), 23-38.

72. Hou, Q.; Grijpma, D. W.; Feijen, J., Porous polymeric structures for tissue engineering prepared by a coagulation, compression moulding and salt leaching technique. *Biomaterials* **2003,** 24, (11), 1937-47.

73. Murphy, W. L.; Dennis, R. G.; Kileny, J. L.; Mooney, D. J., Salt fusion: an approach to improve pore interconnectivity within tissue engineering scaffolds. *Tissue Eng* **2002,** 8, (1), 43-52.

74. Oh, S.; Kang, S.; Kim, E.; Cho, S.; Lee, J., Fabrication and characterization of hydrophilic poly(lactic-co-glycolic acid)/poly(vinyl alcohol) blend cell scaffolds by melt-molding particulate-leaching method. *Biomaterials* **2003,** 24, 4011-21.

75. Weigel, T.; Schinkel, G.; Lendlein, A., Design and preparation of polymeric scaffolds for tissue engineering. *Expert review of medical devices* **2006,** 3, (6), 835-51.

76. Seitz, H.; Rieder, W.; Irsen, S.; Leukers, B.; Tille, C., Three-dimensional printing of porous ceramic scaffolds for bone tissue engineering. *J Biomed Mater Res Part B Appl Biomater* **2005,** 74, (2), 782-8.

77. Nam, Y. S.; Yoon, J. J.; Park, T. G., A novel fabrication method of macroporous biodegradable polymer scaffolds using gas foaming salt as a porogen additive. *J Biomed Mater Res* **2000,** 53, (1), 1-7.

78. Nublat, C.; Braud, C.; Garreau, H.; Vert, M., Ammonium bicarbonate as porogen to make tetracycline-loaded porous bioresorbable membranes for dental guided tissue regeneration: failure due to tetracycline instability. *J Biomater Sci Polymer Edn* **2006,** 17, (12), 1333-46.

79. Taboas, J. M.; Maddox, R. D.; Krebsbach, P. H.; Hollister, S. J., Indirect solid free form fabrication of local and global porous, biomimetic and composite 3D polymer-ceramic scaffolds. *Biomaterials* **2003,** 24, (1), 181-94.

80. Subbiah, T.; Bhat, G. S.; Tock, R. W.; Parameswaran, S.; Ramkumar, S. S., Electrospinning of nanofibers. *J Appl Polym Sci* **2005,** 96, 557.

81. Pham, Q. P.; Sharma, U.; Mikos, A. G., Electrospinning of polymeric nanofibers for tissue engineering applications: a review. *Tissue Eng* **2006,** 12, (5), 1197-211.

82. Demir, M.; Yilgor, I.; Yilgor, E.; Ermana, B., Electrospinning of polyurethane fibers. *Polymer* **2002,** 43, 3303-09.

83. Vaz, C. M.; van Tuijl, S.; Bouten, C. V. C.; Baaijens, F. P. T., Design of scaffolds for blood vessel tissue engineering using a multi-layering electrospinning technique. *Acta biomaterialia* **2005,** 1, (5), 575-82.

84. Grenier, S.; Sandig, M.; Mequanint, K., Smooth muscle alpha-actin and calponin expression and extracellular matrix production of human coronary artery smooth muscle cells in 3D scaffolds. *Tissue Eng Part A* **2009,** 15, (10), 3001-11.

85. Dubey, G.; Mequanint, K., Conjugation of fibronectin onto three-dimensional porous scaffolds for vascular tissue engineering applications. *Acta Biomaterialia* **2011,** 7, (3), 1114-25.

86. Lin, S.; Sandig, M.; Mequanint, K., Three-dimensional topography of synthetic scaffolds induces elastin synthesis by human coronary artery smooth muscle cells. *Tissue Eng Part A* **2011,** 17, (11-12), 1561-71.

87. Heng, P. W. S.; Chan, L. W.; Wong, T. W., Formation of alginate microspheres produced using emulsification technique. *J Microencapsul* **2003,** 20, (3), 401-13.

88. Lin-Gibson, S.; Cooper, J. A.; Landis, F. A.; Cicerone, M. T., Systematic investigation of porogen size and content on scaffold morphometric parameters and properties. *Biomacromolecules* **2007,** 8, (5), 1511-8.

89. Ratcliffe, A., Tissue engineering of vascular grafts. *Matrix Biol* **2000,** 19, (4), 353-7.

90. Sarkar, S.; Schmitz-Rixen, T.; Hamilton, G.; Seifalian, A. M., Achieving the ideal properties for vascular bypass grafts using a tissue engineered approach: a review. *Med Bio Eng Comput* **2007,** 45, (4), 327-36.

91. Tønnesen, H.; Karlsen, J., Alginate in Drug Delivery Systems. *Drug Development and Industrial Pharmacy* **2002,** 28, (6), 621-630.

92. Fundueanu, G.; Nastruzzi, C.; Carpov, A.; Desbrieres, J.; Rinaudo, M., Physico-chemical characterization of Ca-alginate microparticles produced with different methods. *Biomaterials* **1999,** 20, (15), 1427-35.

93. Poncelet, D.; Neufeld, R. J.; Goosen, M.; Burgarski, B.; Babak, V., Formation of Microgel Beads by Electric Dispersion of Polymer Solutions. *AIChE* **1999,** 45, (9), 2018-2023.

94. Chan, L. W.; Heng, P. W.; Wan, L. S., Effect of cellulose derivatives on alginate microspheres prepared by emulsification. *J Microencapsul* **1997,** 14, (5), 545-55.

95. Chuah, A.; Kuroiwa, T.; Kobayashi, I.; Zhang, X.; Nakajima, M., Preparation of uniformly sized alginate microspheres using the novel combined methods of microchannel emulsification and external gelation. *Colloids and Surfaces A: Physicochem Eng Aspects* **2009,** 351, 9-17.

96. Wan, L. S.; Heng, P. W.; Chan, L. W., Influence of hydrophile–lipophile balance on alginate microspheres. *Int J Pharm* **1993,** 95, (1-3), 77-83.

97. Silva, C. M.; Ribeiro, A. J.; Figueiredo, I. V.; Gonçalves, A. R.; Veiga, F., Alginate microspheres prepared by internal gelation: development and effect on insulin stability. *Int J Pharm* **2006,** 311, (1-2), 1-10.

98. Ma, P. X.; Zhang, R., Synthetic nano-scale fibrous extracellular matrix. *J Biomed Mater Res* **1999,** 46, (1), 60-72.

99. Poncelet, D.; Lencki, R.; Beaulieu, C.; Halle, J. P.; Neufeld, R. J.; Fournier, A., Production of alginate beads by emulsification/internal gelation. I. Methodology. *Appl Microbiol Biotechnol* **1992,** 38, (1), 39-45.

100. Poncelet, D.; Babak, V.; Dulieu, C.; Picot, A., A physico-chemical approach o production of alginate beads by emulsification-internal ionotropic gelation. *Colloids and Surfaces A: Physicochemical Eng Aspects* **1999,** 155, 171-176.

101. Lowery, J. L.; Datta, N.; Rutledge, G. C., Effect of fiber diameter, pore size and seeding method on growth of human dermal fibroblasts in electrospun poly(epsilon-caprolactone) fibrous mats. *Biomaterials* **2010,** 31, (3), 491-504.

102. Gao, J.; Crapo, P. M.; Wang, Y., Macroporous elastomeric scaffolds with extensive micropores for soft tissue engineering. *Tissue Eng* **2006,** 12, (4), 917-25.

103. Bezuidenhout, D.; Davies, N.; Zilla, P., Effect of well defined dodecahedral porosity on inflammation and angiogenesis. *ASAIO J* **2002,** 48, (5), 465-71.

104. Heydarkhan-Hagvall, S.; Schenke-Layland, K.; Dhanasopon, A. P.; Rofail, F.; Smith, H.; Wu, B. M.; Shemin, R.; Beygui, R. E.; MacLellan, W. R., Three-

dimensional electrospun ECM-based hybrid scaffolds for cardiovascular tissue engineering. *Biomaterials* **2008,** 29, (19), 2907-14.

105. Cory, A.; Owen, T.; Barltrop, J.; Cory, J., Use of an aqueous soluble tetrazolium/formazan assay for cell growth assays in culture. *Cancer Commun* **1991,** 3, 207-212.

106. Zhang, S.; Gelain, F.; Zhao, X., Designer self-assembling peptide nanofiber scaffolds for 3D tissue cell cultures. *Semin Cancer Biol* **2005,** 15, (5), 413-20.

107. Li, S.; Lao, J.; Chen, B. P. C.; Li, Y.-s.; Zhao, Y.; Chu, J.; Chen, K.-D.; Tsou, T.-C.; Peck, K.; Chien, S., Genomic analysis of smooth muscle cells in 3-dimensional collagen matrix. *FASEB J* **2003,** 17, (1), 97-9.